Al-Farabi Kazakh National University

UDC: 543.2 (043) On manuscript rights

KAPAR ANEL AMANGELDYKYZY

Modeling the processes of solid-phase microextraction of organic compounds from environmental objects

8D05301 – Chemistry

Thesis submitted in fulfillment of the requirements
for the degree of
Doctor of Philosophy (PhD)

Scientific supervisors:

Ph.D., Orazbayeva D.S.

Ph.D., Associate Professor
Iowa State University, USA
Koziel J.A.

The Republic of Kazakhstan

Almaty, 2024

TABLE OF CONTENTS

NORMATIVE REFERENCES **4**
LIST OF SYMBOLS AND ABBREVIATIONS **5**
INTRODUCTION **8**
1 LITERATURE REVIEW **14**
1.1. Hazards of VOCs and importance of environmental monitoring 14
1.2 Tools and methods of environmental monitoring 18
1.3 Theoretical and technical basis of solid-phase microextraction 22
1.4 Optimization of SPME parameters 26
1.5 Modelling of SPME 29
1.5.1 COMSOL Multiphysics® for SPME simulation 29
1.5.2 Physical and mathematical models of SPME 30
2 DEVELOPMENT OF COMPUTATIONAL MODEL FOR PREDICTING THE EFFECT OF TEMPERATURE ON SOLID-PHASE MICROEXTRACTION OF VOLATILE ORGANIC COMPOUNDS FROM AIR USING COMSOL MULTYPHYSICS®
2.1 Introduction 33
2.2 Methods 35
2.2.1 General modeling parameters 35
2.2.2 Estimation of coating-air distribution constant 39
2.2.3 Estimation of diffusion coefficients in air 39
2.2.4 Estimation of diffusion coefficients in the PDMS coating 39
2.3 Experimental 40
2.3.1 Reagents and materials 40
2.3.2 Parameters of gas chromatography-mass spectrometry (GC-MS) analysis 40
2.3.4 Experimental study of the effect of the temperature on extraction profiles of analytes 42
2.4 Results and discussion 42
2.4.1 Selection of the method for estimating diffusion coefficients in air 42
2.4.2 Diffusion coefficients in the PDMS coating 44
2.6 Chapter conclusion 48
3 MODELING HEADSPACE SOLID-PHASE MICROEXTRACTION OF VOLATILE ORGANIC COMPOUNDS FROM WATER SAMPLES WITH POROUS COATINGS USING FINITE ELEMENT ANALYSIS 49
3.1 Introduction 49
3.2 Theory 49
3.2.1 Adsorption from headspace to a porous coating 50
3.2.2 Mass transport in a porous coating 50
3.2.3 Mass transport in aqueous phase and partitioning between headspace and aqueous phase 50
3.2.4 Estimation of K_{hw} (HLC) values 52
3.3 Method 53
3.3.1 General modeling parameters 53

3.3.2 Comparison of simulated and experimental profiles 57
3.3.3 Application of the developed model for optimization of extraction parameters 58
3.3.4 Optimization of incubation time 59
3.4 Results and discussion 59
3.4.1 Comparison of simulated and experimental profiles 59
3.4.2 Application of the developed model for optimization of extraction parameters 60
3.4.3 Optimization of preincubation time 62
3.5 Conclusion on the section 62
4 DEVELOPMENT AND APPLICATION OF COMPUTATIONAL MODELS FOR SIMULATING HEADSPACE SOLID-PHASE MICROEXTRACTION OF ORGANIC COMPOUNDS FROM SOIL 64
4.1 Introduction 64
4.2. Method 64
4.2.1 Modeling of HSSPME 64
4.2.2 Modeling of pre-incubatio 66
4.3 Results and Discussion 67
4.3.1 Extraction profiles obtained during the modeling 67
4.3.2 Effect of sample mass under atmospheric pressure 67
4.3.3 Effect of sample mass under vacuum conditions 68
4.3.4 Optimization of pre-incubation time 69
4.4 Chapter conclusion 70
CONCLUSION 71
REFERENCES 73

NORMATIVE REFERENCES

In this dissertation, references are made to the following standards:

EPA Method 8270 Semivolatile Organic Compounds by Gas Chromatography / Mass Spectrometry (GC/MS)

MUC 4.1.618-96. Guidelines for chromato-mass spectrometric determination of volatile organic substances in atmospheric air.

Method EPA-RCA 8270D. Semivolatile organic compounds by GC-MS.

Method EPA-EAD 1625. Semivolatile organic compounds by isotope dilution GC-MS.

LIST OF SYMBOLS AND ABBREVIATIONS

The following symbols and abbreviations are used in this research report:

B	longitudinal diffusion in mobile phase
BTEX	benzene, toluene, ethylbenzene, o-xylene
Car/PDMS	Carboxen/polydimethylsiloxane
C_a	equilibrium concentration of an analyte in air
C_f	equilibrium concentration of an analyte in coating
C_G *and* C_L	resistance to mass transfer in the mobile and stationary phases
C_h	boundary concentration of an analyte in the headspace
C_s	equilibrium concentration of an analyte in soil
C_w	boundary concentrations of an analyte in water
CMP	COMSOL Multiphysics®
CPCMRA	Center of Physical-Chemical Methods of Research and Analysis
d	thickness of the stationary phase
D_0	pre-exponential factor for the analyte-polymer system
D_a	diffusion coefficient in air
D_m	diffusion coefficient in mobile phase
D_s	diffusion coefficient in PDMS
D_w	diffusion coefficient in water
E_a	activation energy of diffusion
u	linear flow velocity,
USA	United States of America
FID	flame ionization detector
FV	free volume theory
IGC	inverse gas chromatography
H	theoretical plate height
ΔH	heat of vaporization
HSSPME	headspace solid-phase microextraction
HPLC	high-performance liquid chromatography
GC	gas chromatography
GC-MS	gas-chromatography-mass spectrometry
k	retention factor
K_{hw}	Henry's law constant
K_L	flux coefficient
K_{fa}	distribution constant between headspace and coatig

k_h и k_w	exchange constants for the headspace and water
K_p	coatKing-headspace distribution constant
LOD	limit of detection
LOQ	limit of quantification
LSER	linear solvation energy relationship
LTPRI	linear temperature programmed retention indices
j	compressibility
M_A и M_B	molecular weight of an analyte A and B
M (H_2O)	molecular weight of water
M_h	molecular weight of a gas in headspace
MI-PTRMS	membrane-introduction proton-transfer reaction mass spectrometry
MSD	mass spectrometric detector
N	number of carbon atoms
P	pressure
PDMS	polydimethylsiloxane
p_i	absolute pressure in GC injector
p_o	atmospheric pressure in the laboratory
R	gas constant
r	internal radius of a column
RMSD	lowest values of root-mean-square deviation
S	stirring rate
SIM	selected ion monitoring
SPME	solid-phase microextraction
T	temperature
t_R	retention time
$t_{R(a)}$	retention time of an analyte
t_{R0}	void time
$t_{R(N)}$ и $t_{R(N+1)}$	retention times of *n*-alkanes eluting before and after the analyte
TWA	time-weighted average
V_a	molar volume of an analyte at its normal boiling point
Vac-HSSPME	vacuum headspace solid-phase microextraction
V_A и V_B	molecular diffusion volumes of A and B
V_C	analyte critical volume
$V_{current}$	current velocity
VOCs	volatile organic compounds
x_i	time

ε	porosity of coating
y_i	detector response at x_i
Ω_D	collision integral
σ_{AB}	Lennard-Jones collision diameter
φ	association parameter of the solvent
μ	dynamic viscosity of water

INTRODUCTION

Characterization of the work

This study is aimed at the improvement of the efficiency of the development of analytical methods for environmental objects based on solid-phase microextraction using computer modeling.

The relevance of the research topic

Environmental pollution caused by toxic chemicals has significant adverse effects on both human health and the economy. Environmental monitoring serves as the foundation for estimating and identifying sources of risk, as well as for making decisions regarding environmental pollution. Establishing a proper system of environmental monitoring is a highly complex task that demands substantial financial and human resources, particularly in developing countries like Kazakhstan.

Environmental regulations in Kazakhstan mandate the use of certified analytical methods, many of which are outdated and involve costly and labor-intensive sample preparations, especially for organic pollutants. The current high cost of analysis can be mitigated by developing cost-effective methods. Traditional environmental analyses are expensive primarily due to time-consuming sample preparations. However, modern equipment allows for continuous and fully automated sample analysis without significant cost escalation.

Headspace (HS) solid-phase microextraction (SPME) is considered one of the most promising sample preparation methods for identifying organic pollutants in environmental samples due to its simplicity, environmental friendliness, automation, and ability to achieve low detection limits at a minimal cost of analysis. Nonetheless, optimizing SPME parameters demands extensive experimental efforts and expenses. Achieving a proper balance between detection limits and accuracies requires thorough optimization of approximately ten extraction parameters (such as fiber coating type, coating dimensions, extraction temperature, extraction time, pH, amount of salt added to a sample, sample/headspace ratio, agitation/stirring rate, and pressure in a vial) and desorption parameters (desorption temperature and time). This process can be time-consuming, costly, and complex. Optimization proceeds step by step, during which it is impossible to explore all parameter combinations. Method developers often prioritize maximizing analyte responses over accuracy during optimization due to its complexity. Consequently, SPME-based methods for various analytes and sample types are not yet widely available.

Simulation of the SPME process is an effective tool for developing and optimizing analytical methods. However, models to simulate the effects of many important extraction parameters (such as extraction temperature, pressure, ionic strength of water

samples, and soil moisture) are still unavailable, and method optimization still requires significant experimental work and expense from method developers. By incorporating the effects of these parameters into a computational model, there is great potential to replace experimental optimization.

The aim of the study is to establish theoretical and computational basis for developing SPME models to enhance the optimization process and predicting the optimal parameters of SPME for various analytes and samples without conducting elaborative experimental optimization. This goal was achieved during the development of new computational models for simulation of SPME of VOCs from air, water and soil.

The following tasks were set to accomplish the aim of the study:

1) To develop mathematical and physical models of processes taking place during SPME of VOCs from air, water and soil;

2) To determine diffusion coefficients and distribution constants of analytes in different matrices;

3) To evaluate the accuracy of different prediction methods for calculating the diffusion coefficients of VOCs in air, water and soil using experimental and empirical data;

4) To develop a computational model of SPME of BTEX from air for optimization of an extraction time of analytes at different temperatures, pressures, sample volumes and geometries at constant or changing conditions.

5) To develop a computational model of SPME of BTEX from water for optimization of stirring speed, fiber insertion depth, pressure, sample volume and the concentration of added salt.

6) To develop a computational model of SPME of BTEX from soil for optimization of sample mass, location of the fiber, extraction time and pressure.

Objects of the research: computational models of processes occurring during solid-phase microextraction of volatile organic compounds from air, water, soil.

Subject of the research: the optimization of SPME of VOCs from air, water, soil using COMSOL Multiphysics®.

The methods of the research. The scientific method was used to disclose knowledge gaps, formulate research questions and hypotheses, design experiments in this study. Computational program COMSOL Multiphysics ® was used for construction of SPME models and SPME optimization. Gas chromatography–mass spectrometry (GC-MS) was used for signal measurement during the optimization and development of analytical methods.

The scientific novelty of the research

1) Diffusion coefficients of BTEX in the PDMS fiber using capillary inverse gas chromatography were established for the first time.

2) The effect of diffusion in PDMS coating, distribution constants, and extraction

temperature of SPME of BTEX from air were evaluated and established for the first time using finite element analysis.

3) The effect of stirring rate, fiber insertion depth, sample volume, concentration of added salt and pressure conditions on the performance of SPME of BTEX by Car/PDMS coating from water using finite element analysis were evaluated and established for the first time.

4) The effect of sample mass, pressure in the system, distribution constant on SPME of benzene by Car/PDMS coating from soil using finite element analysis were established for the first time.

Validity and reliability of the results obtained. The results obtained are valid and reliable because all experiments were conducted with one or two independent variables while the other variables were held constant. The dependent variables depicted the main parameters of the methods such as precision, recovery, analyte responses, limits of detection and quantification, and reproducibility. All measurements were performed in two to four repetitions. Gas chromatography with mass spectrometric detection was used to achieve sensitive and selective identification and separation of VOCs.

The theoretical and practical importance of the dissertation.

This research improved the theory of solid-phase microextraction behind the optimization parameters of the method by using computer simulation. Computational models of solid-phase microextraction of volatile organic compounds from environmental objects were developed. The developed models make it possible to optimize the SPME parameters to increase the extraction efficiency and reduce the analysis time. The models can be used to generate complete extraction profiles at various temperatures, pressures, sample volumes and geometries under constant or varying conditions. Almost all input data can be found in the scientific literature and databases or can be predicted using the proposed computational methods. In addition, estimation methods were performed to generate the predicted values of diffusion coefficient of VOC in air, distribution coefficient in air and soil. The only experimental step that the end users of the developed model must perform is the determination of the diffusion coefficients in the fiber using reversed gas chromatography (if not available in the literature). Training material and simulation videos have been developed to enable end users to model themselves and extract extraction profiles by incorporating data from their subjects. All developed computer models were validated experimentally and compared with the results of other studies and experiments.

The main statements to be defended:

1) The computational optimization of temperature and time of solid-phase microextraction of VOCs from air can be achieved using prediction techniques of Fuller method for diffusion coefficients in air, LTPRI indices and van't Hoff equation for estimation of distribution constants between headspace and fiber, and inverse gas

chromatography for diffusion in PDMS with RMSDs in the range between 4.5% to 13.3% compared to obtained experimental extraction profiles at 298K.

2) Increasing the coating-air distribution constant from 1000 to 10000 at constant temperature and diffusion coefficient in PDMS coating equal to 10^{-11} m^2s^{-1} results in 43% increase of equilibration time.

3) Southworth approach allows obtaining simulated HSSPME profiles of BTEX from water by Car/PDMS coating, which are closest to experimental profiles compared to other approaches with RMSD in the range 8.8-10%.

4) Using vacuum and increasing stirring speed from 500 to 1000 and 2000 RPM allows to decrease equilibration time ($t_{95\%}$) of benzene using 85 μm Car/PDMS fiber by 2.5 (48%) and 3.8 min (71%), respectively.

5) Equilibrium in the system with Vac-HSSPME (0.0313 atm) can be reached 42-43 times faster compared to HSSSPME at all studied distribution constants and sample masses of benzene extraction by Car/PDMS coating.

The main results of the study:

1) The computational optimization of temperature and time of solid-phase microextraction of VOCs from air can be achieved using prediction techniques of Fuller method for diffusion coefficients in air, LTPRI indices and van't Hoff equation for estimation of distribution constants between headspace and fiber, and IGC for diffusion in PDMS with RMSDs in the range between 4.5% to 13.3% compared to obtained experimental extraction profiles of BTEX at 25°C and 40°C. Diffusion in the coating is a limiting stage in the extraction process at lower distribution constant between coating and air. When coating-air distribution constant equals to 10^3 the decrease of diffusion in the PDMS coating from $2 \cdot 10^{-9}$ m^2 s^{-1} to 10^{-11} m^2 s^{-1}, results the increase of the equilibration time from 6.5 to 32.6 seconds for extracting 80% of benzene at 25°C. At coating-air distribution constant equals to 10^5 similar decrease diffusion in the PDMS coating results increase from 46 to 66 seconds of equilibration time of benzene.

2) Vac-HSSPME provides faster equilibration compared to HSSPME for all (with any K_{fh} and HLC) VOCs from water at 298K under ideal stirring conditions by Car/PDMS coating. Increase of stirring speed from 500 to 1000 and 2000 RPM allows to decrease equilibration time (t95%) of benzene extraction from water by 2.5 (48%) and 3.8 min (71%), respectively under vacuum conditions. Southworth approach for estimating mass transfer coefficients at water-headspace boundary allows computational optimization of extraction time of SPME from water with RMSDs in the range 8.8-10% compared to experimental extraction profiles.

3) Equilibration time of benzene extraction by Car/PDMS coating from dry soil at Vac HSSPME (0.0313 atm) can be reached faster at 2.3 min compared to traditional HSSSPME, where equilibrium under atmospheric pressure (1 atm) is reached at 97 min Equilibration

time ($t0_{.95}$) depends on both sample mass and soil-headspace distribution constant of the analyte. For the small sample masses less than 5 g, and soil-headspace distribution constants less than 100, equilibrium in the system can be achieved less than after 1 min of benzene extraction at K_{fh}=150 000 and less than 0.1 min at K_{fh}=8300 by Car/PDMS porous coating at 298K under vacuum conditions. For soil-headspace distribution constants more than 10^5 equilibration at the same time can be achieved for the sample mass of 10 g.

The accordance of the dissertation theme to a plan of the research work and various State programs. The dissertation theme complies with the plan of the researchwork. The research work was conducted under the projects funded by the Ministry of Education and Science of Kazakhstan:

-"Efficient development of environmental and analytical methods based on headspace solid-phase microextraction using computer simulation" (No. AP08052684, 2020-2022).

The author's contribution to the research consists of preparation and analysis of literature review, planning and performing the experiments, interpreting the obtained data, and integrating them into the final results and analytical methods.

Presentation of the practical results. The main results of the work were presented at the following international conferences:

- 1st European Sample Preparation Conference (Online event, 11-12 March, 2021)

Publications. The results of this research were published in 4 scientific papers, including:

- One article in the international scientific journal indexed in Scopus and Web of Science (Thomson Reuters/Clarivate Analytics) databases with impact-factor 6.911;
- Two articles in journals recommended by the Committee for Control in Education and Science of the Ministry of Education and Science of the Republic of Kazakhstan;
- One abstract of international scientific conference (online event)

Description of contribution of the PhD student to each publication

1) Kapar A. et al. Modeling the effect of temperature on solid-phase microextraction of volatile organic compounds from air by polydimethylsiloxane coating using finite element analysis // Anal Chim Acta., 2022. Vol. 1195. P. 339431. https://doi.org/10.1016/j.aca.2022.339431 (Validation, formal analysis, investigation, writing original draft, writing review and editing.)

2) Muratuly A., Kapar A., Kenessov B. Modeling headspace solid-phase microextraction of volatile organic compounds from water samples with porous coatings using finite element analysis // Advances in Sample Preparation, 2022. Vol. 3. https://doi.org/10.1016/j.sampre.2022.100030 . (Validation, writing original draft, writing review)

3) Kenessov B., Kapar A. Optimization of headspace solid-phase microextraction of volatile organic compounds from dry soil samples by porous coatings using COMSOL

Multiphysics // Chemical Bulletin of Kazakh National University. Center of Physical Chemical Methods of Research and Analysis, 2022. № 4. P. 4–12. https://doi.org/10.15328/cb1300 (Validation, writing review and editing)

The structure of the dissertation. The dissertation is presented in 84 pages and contains 14 tables, 21 figures and 147 references. The dissertation consists of introduction, four chapters, conclusion, list of references.

Acknowledgments. The author would like to express her sincerest gratitude to supervisors, Ph.D Dina Orazbayeva and Dr. Jacek Koziel, also for co-supervisor Professor Bulat Kenessov for the continued support, for sharing with the invaluable ideas and advice, as well as for the vivid mentoring and encouragement provided throughout this work. I would like to extend special thanks to Professor Levent Pelit for his supervision, support, and for making me feel at home during my entire internship at the Department of Chemistry at EGE University.

I also want to acknowledge the contributions of my family, especially my husband and daughter, for their support and for allowing me time to conduct my Ph.D. research. Additionally, I am very thankful to the research group alumni of the Ecology of Biosphere Laboratory at the Center of Physico-Chemical Methods of Research and Analysis (Al-Farabi Kazakh National University) for their assistance. I especially appreciate the support of my research team members, Balgyn Dyssenkulova, Aset Muratuly, and Nadezhda Bakaikina, throughout my Ph.D. research period.

1 LITERATURE REVIEW

1.1. Hazards of VOCs and importance of environmental monitoring

The study of volatile organic compounds (VOCs) is becoming increasingly important due to their impact on global environmental conditions and human well-being. Besides their persistence and accumulation in the environment, VOCs contribute to heightened greenhouse effects and associated ozone depletion. VOCs enter the atmospheric air during photochemical reactions, photolysis, and from biogenic and anthropogenic sources. Due to their high volatility, VOCs mainly contaminates groundwater than surface water. Vapors of VOCs through air streams pollute the soil [1].

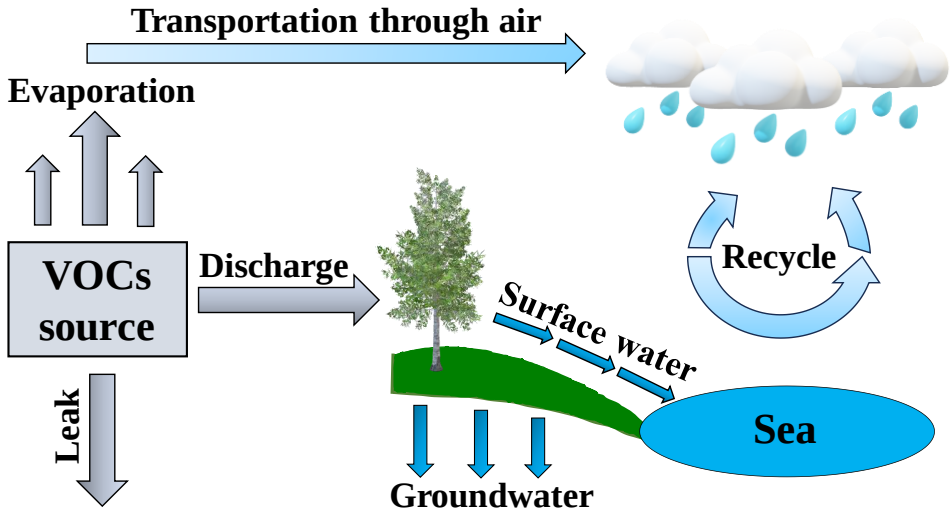


Figure 1 – Distribution of VOCs in environment [2]

In relatively unpolluted waters, VOCs constitute approximately 10% of the total dissolved organic carbon, while their concentrations are much higher in raw waters originating from various human-related sources [3]. When present in water, the behavior of VOCs is influenced by their physicochemical properties, such as dilution, toxicological changes, and biodegradation, which play crucial roles in their stability and concentration levels. The BTEX group, which includes benzene, toluene, ethylbenzene, and xylene, are the most frequently measured VOCs [4]. BTEX primarily originate from sources such as motor vehicle gasoline, paints, various industrial processes, and raw materials used in industries [5]. These constituents are widely present in environmental samples like water, air, and soil, increasing the potential for human exposure through ingestion, inhalation, or skin absorption, thereby raising health risks.

Benzene is a substance known to cause cancer, as stated by the US Environmental Protection Agency in 2012. Therefore, neither the World Health Organization nor the US EPA provide any safe exposure limits for benzene [6]. The European Union has implemented the most rigorous standards for benzene, with legislation that sets a maximum

average annual concentration of 5 μgm^{-3}. Originally obtained from coal tar in 1800, benzene is now mainly extracted from petroleum. It can be found in petroleum, gasoline, and cigarette smoke, as well as in gas emissions from forest fires and volcanic eruptions. Benzene is widely used in the chemical industry to produce various compounds, such as styrene, cumene, and cyclohexane. Additionally, it is employed to manufacture lubricants, dyes, detergents, drugs, and pesticides [7]. Benzene is one of the top 20 chemical compounds produced in the US. The increase in the concentration of benzene in the air is associated with emissions from coal and oil combustion, waste and storage of benzene, vehicle exhaust gases and fuel evaporation from gas stations [8]. Short-term exposure to benzene on the human body leads to drowsiness, headaches and dizziness, long-term exposure can cause leukemia. The impact of benzene, even at low concentrations, has a negative effect on the cells of the human body [9].

Toluene is an air pollutant with high potential danger [10]. It appears as a clear, colorless liquid that has a distinct odor. Toluene is present in raw petroleum, the tolu tree, and is generated from the combustion of organic matter, such as wood, coal, and petroleum products. In urban atmospheres, vehicle exhaust fumes are the leading cause of toluene emissions, and it is also released into the air from fuel evaporation at warehouses, gas stations, and service stations. The highest concentration of toluene is typically found in indoor air, particularly when household products such as paints, solvents, and adhesives containing toluene are used or during smoking [11].

Ethylbenzene is a flammable liquid with a colorless appearance and a gasoline-like odor [12]. It is present in coal tar and petroleum and is commonly found in industrial products like inks, pesticides, and paints [13]. Ethylbenzene is predominantly used as a raw material in the production of styrene, as well as a solvent and fuel additive. High concentrations of ethylbenzene in the air may cause irritation to the eyes and throat. Exposure to relatively low concentrations of ethylbenzene for several days to weeks has been observed to cause irreversible hearing damage in animals [14] .

Xylene is a synthetic liquid with a sweet scent. The industrial production of xylene is derived from petroleum, while it is also naturally present in crude oil and coal tar [15]. Xylene is widely used in the production of rubber and leather, synthetic fibers, plastics, and printing. Xylene easily evaporates and is combustible [16]. Xylene enters the environment through transportation, storage, and production. Soil microorganisms can also degrade it, and small amounts are absorbed by plants and animals. Short-term exposure to high concentrations of xylene can lead to headaches, muscle coordination issues, dizziness, skin, eye, nose, and throat irritation, breathing difficulties, memory impairment, stomach discomfort, liver and kidney dysfunction, confusion, and motor coordination changes [17].

BTEX is released into the environment through various sources, namely pyrogenic, petrogenic, and processed products [18]. Pyrogenic BTEX is formed when organic matter

is exposed to high temperatures through processes such as pyrolysis, which includes the combustion of coal or thermal cracking of petroleum. Incomplete combustion of coal or wood can result in the release of a substantial amount of VOCs, with BTEX accounting for approximately 61.1–94.8% [19]. BTEX constituted 59% (w/w) of gasoline pollutants, and petrochemical plants were responsible for 80% of VOC emissions, primarily BTEX [20].

The building materials industry and chemical processed products represent the third significant source of BTEX compounds. In architectural or furnishing coatings, BTEX compounds, particularly BTX, accounted for 7%, 19%, and 13% of total VOCs respectively [21]. BTEX can be derived from the conversion of raw oil and gas at high temperatures, providing essential materials for the petrochemical industry and playing a crucial role in chemical development. Biomass, such as lignin and cellulose/hemicellulose, can be depolymerized to produce BTEX due to its abundant aromaticity, making it an ideal alternative for BTEX production [22].

The primary sources of BTEX in natural waters are sewage discharge, oil leaks, and water transportation. The levels of BTEX can be influenced by factors such as temperature and precipitation. A study by Moliner-Martínez et al. examined the impact of seasonal temperature and precipitation on BTEX levels in natural waters [23]. The findings revealed that temperature and precipitation have an effect on BTEX levels, with a correlation coefficient of 0.8. When there is an increase in water discharge and temperature, the concentration of pollutants tends to decrease. In the general environment, benzene primarily accumulates in the air (99.9%) rather than in water or soil. BTEX levels in the air are influenced by factors such as temperature, diffusion, and distance from the source. Generally, lower concentrations of BTEX are observed during warmer months. For example, in Beijing, BTEX concentrations in the air were 1.5 times higher in November compared to July [24]. The occurrence of an inverse temperature layer during winter prevents the dilution of pollutants, leading to increased BTEX concentrations in the atmosphere. [25–27].

Understanding the spatial distribution of BTEX in the environment, including the atmosphere, water, and soil, is crucial for effective management and implementation of control strategies. A summary of representative distributions of BTEX in air and water can be found in Table 1. It is important to note that BTEX levels vary considerably between urban streets and urban industrial sites. The concentration of BTEX at industrial locations is heavily influenced by industrial activities. Dehghani et. al conducted a study on the source apportionment of BTEX compounds at an industrial site in Tehran, Iran [28]. They identified several major sources, including solvent and paint sources (5%), vehicle exhaust emissions (29%), rubber and plastic manufacturing (26%), leather industry (18%), and unknown sources (20%). Gas stations and municipal solid waste transfer stations are the primary sources of BTEX pollution. In densely populated areas, relocating these stations

outside the urban area could be a potential approach to minimize public exposure. Additionally, the levels of BTEX in the atmosphere differ significantly across different regions of China and no less in Kazakhstan [22, p.125, 29, p.1].

Based on the soil texture, which refers to the composition of sand, silt, and clay, the soil can be broadly classified into 12 categories: sand, loamy sand, sandy loam, sandy clay loam, sandy clay, clay, clay loam, silty clay, silty clay loam, loam, silt loam, and silt. In a study by Owabor et al., it was observed that BTEX reached equilibrium more quickly in sand due to its higher bulk porosity and permeability. On the other hand, clay, with its larger surface area, absorbed more BTEX compared to sand [30]. Varona-Torres et al. investigated the relationship between pollutant emissions from industrial sites and the presence of BTEX in soil in the Eagle Ford shale region of southern Texas [31]. The solubility of BTEX in water allows the pollutants to persist in soils with a larger liquid phase for a longer period, rather than migrating downward or volatilizing in dry soils. They collected 276 soil samples, including sand, loamy sand, sandy loam, loam, and sandy clay loam. Interestingly, the study revealed that the total BTEX concentration and the distribution of individual BTEX constituents were not influenced by the proximity to the emissions source. The density of the emission source, distance from the source, and prevailing wind also had no significant impact on the BTEX contents in the soil. Instead, soil texture appeared to have the most significant influence on the overall BTEX concentration.

Table 1 – BTEX distributions in air and water in different regions

Country, city	Sample	Total BTEX concentrations, $\mu g\ m^{-3}$	Reference
Kazakhstan, Almaty	Urban air	135 (Spring)	[29]
France, Orlean	Urban air	2.3 (Spring)	[26]
		3.6 (Winter)	
Ethiopia, Mekelle	Urban air	36	[32]
Vietnam, Ha Giang	Urban air	47	[33]
Japan, Yokohama	Petrochemical plant air	29	[34]
Iran, Tehran	Urban air	40.6	
Iran, Shiraz	Contaminated surface water	100 (B); 150 (E); 320 (X)	[35]

Pakistan	Produced water from a gas field	15.7 (B); 14 (T); 29 (E); 2.01 (m and p-Xylene);	[36]
Fortaleza, Coast, Brazil	Environmental aqueous matrices	486	[37]

Hazardous impact of BTEX on human health requires a systematic monitoring of VOC concentration in environmental objects not to exceed the maximum permissible concentration (MPC). The maximum permissible concentration of BTEX demonstrated on table 2 exceed the MPC according to the legislation of Kazakhstan from 10 to 15 times. Based on the statistics Almaty is considered as the 8th most polluted city by BTEX in 20 major cities worldwide [29, p.2]. Such exceeding requires development of cost effective and quick monitoring methods for BTEX in environmental samples not only in Kazakhstan, but also for the whole world.

Table 2 – Physico-chemical properties of BTEX [38]

Compound	Formula	Mol. Wt., g mol $^{-1}$	Boiling point, ^{o}C	Density g cm^{-3}	log K_{ow}	Half-life, h	MPC in air mg dm^{-3}	Hazard class
Benzene	C_6H_6	78,11	80,1	0,88	2,13	209	0,01	I
Toluene	C_7H_8	92,13	110,6	0,87	2,73	43	0,5	IV
Ethylbenzene	C_8H_{10}	106,17	136	0,87	3,15	36	0,02	II
o-Xylene	C_8H_{10}	106,16	144,4	0,88	3,16	19	0,05	III

1.2 Tools and methods of environmental monitoring

Instrumental analysis plays a pivotal role in environmental monitoring by providing precise and sensitive measurements of various pollutants and contaminants in air, water, soil, and other environmental matrices. Advanced instrumentation allows for analysis and continuous data collection, facilitating early detection of environmental hazards and assessment of pollution levels. Additionally, instrumental analysis aids in compliance monitoring with environmental regulations and supports environmental risk assessment and remediation strategies. To gain a comprehensive understanding of the occurrence and behavior of VOCs, analytical techniques capable of detecting and quantifying them at environmental background levels (micrograms per liter and nanograms per liter) are vital. One of the most used techniques in environmental monitoring is gas chromatography, which is based on the differential distribution of sample components between a stationary phase and a mobile gas phase within a chromatographic column. Gas chromatography coupled

with mass spectrometry (GC-MS) is a widely employed in scientific research for its high resolution and sensitivity [39].

Analyzing environmental water samples presents challenges due to the diverse range of analytes, their varying concentrations, and the complex matrix in which they are found. Consequently, the selection of appropriate methods for sample enrichment, determination, isolation, and quantification should depend on the nature of the sample [40].

Sample preparation is a crucial step before conducting qualitative and quantitative analysis, and it directly impacts the accuracy, precision, reproducibility, and limit of detection (LOD) of the method. Effective sample preparation methods are employed to eliminate potential interferences that could obscure trace substances or concentrate target analytes from complex matrices. These methods are designed to extract compounds of interest and align with the requirements of detection techniques. As new technologies and methods continue to evolve, sample pretreatment techniques are continuously advancing. Table 3 provides a comprehensive overview of the sample pretreatment methods utilized for the extraction, purification, and concentration of BTEX since 2010.

Table 3 – Summary of sample preparation techniques of BTEX since 2010

Sample matrix	Sample preparation	Method of analysis	References
Water	UA-DLLME	GC-FID	[41]
Water	SPME	GC-FID	[42]
Water	Ultrasound-assisted emulsification microextraction	GC-FID	[43]
Soil	SPME	GC-FID	[44]
Air	Diffusive sampling	GC-FID	[45]
Water and soil	SPME	GC-FID	[46]
Water	SPME-DLLME	GC-FID	[47]
Soil	NTD	GC-FID	[48]
Water	SPME	GC-FID	[30][49–51] [50]
Soil	Sonification method	UFGC-FID	[52]
Air	Passive sampling	GC-FID	[53]
Water	SPME	GC-MS	[54]
Indoor air samples	SPME	GC-MS	[55]
Soil matrices	QuEChERS	GC–MS	[56]

Water	MSPE	GC-MS	[57]
Air		APCI-MS/MS	[58]
Water	DLLME	GC-MS	[59]
Air	SPME	GC-MS	[60]
Air		Transportable GC-PID, ATD-GC–MS, ATD-GC-FID	[61]
Soil	SLE (RTILs)	GC-MS	[62]
Soil	PC-HS-SPME	GC-FID	[63]
Air	Passive sampling	TD-GC-FID	[45]
Water	SPME	GC-MS	[64]
Water	SPME	GC-FID	[65]

The accurate and reliable analysis of BTEX in environmental matrices is common for assessing the potential risks to human health and the environment. However, the complex nature of these matrices presents significant challenges in sample preparation. To achieve reliable results, appropriate sample preparation techniques are required to extract and concentrate BTEX compounds efficiently while minimizing matrix interferences. Instrumental methods of analysis take an equally important role in the analysis of environmental objects.

Air sampling techniques for BTEX analysis typically involve the use of sorbent tubes or passive sampling devices. Sorbent tubes packed with specific sorbents, such as Tenax TA, are widely used for active air sampling. Passive sampling techniques, such as diffusive samplers, offer advantages in terms of ease of use and low-cost, but may have limitations in terms of accuracy and sensitivity [66] . Diffusive sampling is a commonly employed method for collecting BTEX compounds in gaseous samples, such as atmospheric air. This technique is preferred in air pollution monitoring due to its advantages of being cost-effective, easy to operate, and offering high spatial resolution [45]. Scheepers et al. conducted a study to assess children's exposure to BTEX by employing personal air sampling using diffusive samplers and analyzing end exhaled air. The advantage of this study was the simplicity of the sampling process without the need for complex pretreatment, and it ensured a pollution-free sampling procedure [53]. Typically, carbon disulfide (CS2) is utilized as an organic reagent to release the analytes retained on the sorbent bed of the passive sampler. Subsequently, the extracted samples were directly transferred to the detector, which saved time and reduced labor costs.

For BTEX analysis in water, liquid-liquid extraction (LLE) and solid-phase extraction (SPE) are commonly employed techniques. LLE involves the partitioning of BTEX compounds between an organic solvent and water, while SPE employs solid sorbents to

retain and elute the target analytes. Both techniques have shown good performance, although SPE is often favored due to its simplicity, reproducibility, and compatibility with automation [67]. Headspace extraction is commonly utilized for extracting BTEX compounds in liquid samples. Fakhari et al. developed a rapid and straightforward HS extraction method for the pretreatment of BTEX compounds in water and wastewater samples. By controlling parameters like extraction time, salt addition, stirring rate, and sample volume, satisfactory relative recoveries were achieved for well water (88-105%) and wastewater (84-98%) samples [68]. Furthermore, HS extraction has also been applied as a pretreatment method for solid samples. Zhou et al. employed HS sampling for on-site analysis of BTEX in soils. In this process, a vial containing 5 g of soil was supplemented with a sodium chloride solution (26%), and the gas from the headspace was subsequently extracted and analyzed. After optimization, the recovery of different analytes ranged from 87.2 to 105.1%, with a precision of 5.3 to 7.8% [44].

Sample preparation for BTEX analysis in soil typically involves extraction techniques, such as Soxhlet extraction, accelerated solvent extraction (ASE), or microwave-assisted extraction (MAE). Soxhlet extraction is a classical method that utilizes repeated solvent refluxing, while ASE and MAE employ higher temperatures and pressures to enhance extraction efficiency. Each method has its advantages and limitations, depending on the sample characteristics and target analyte concentrations [69]. Verona-Torres et al. investigated the potential of hydrophilic room temperature ionic liquids (RTILs) as co-solvents in the headspace extraction of BTEX compounds from contaminated soils. The utilization of RTILs as HS solvents is advantageous due to their superior physicochemical properties, including high viscosity, adjustable thermal stability, and a wide liquid range. The research findings demonstrated satisfactory results, with a relative standard deviation (RSD) below 10% and a recovery rate exceeding 80% in the analysis of BTEX compounds. This method offered reduced pretreatment time, improved precision, and enhanced sensitivity compared to the standard method, USEPA 5021A, for the determination of BTEX in soil samples [70]. Nevertheless, various sample preparation techniques are presented for BTEX detection, but not all methods are suitable for all environmental objects. Methods based on HS demonstrated superior results for BTEX preparation in air, soil, water sampling.

Solid-phase microextraction (SPME) is a solvent-free extraction technique derived from solid-phase extraction (SPE). It is an emerging method for the determination of volatile and semi-volatile compounds (VOCs and SVOCs) in different matrices, which has received recognition worldwide. SPME combines sampling, extraction, concentration, and injection into a single step, avoiding the limitations of blocked filter pores [71].

1.3 Theoretical and technical basis of solid-phase microextraction

SPME is based on an extraction of a portion of an analyte from a sample matrix by a micro polymeric coating followed by a desorption of an analyte by a suitable approach, e.g., in an inlet of a gas chromatograph [30]. In the first step, the fiber coating is exposed to the sample and analytes possessing high affinity with the sorbent are extracted by the fiber. In the second step, rapid desorption of extracted analytes into the analytical instrument is performed [31]. Compared to other conventional sample preparation techniques, SPME possesses major significant advantages: simplicity, low detection limit and quickness of operation and high sensitivity [32]. It also offers advantages such as high-throughput capability, simplicity of operation, convenience, and compatibility with chromatographic instruments.

SPME is not an exhaustive, but the equilibrium sample preparation technique. Exhaustive transfer of analytes into the fiber does not occur during SPME [72]. When the concentrations of analyzed substances achieve distribution equilibrium state between the sample and the fiber coating, then it is considered that extraction process is fully completed [67]. This equilibrium can be described by the law of mass conservation:

$$C_0 V_s = C_s^{\infty} V_s + C_f^{\infty} + V_f \quad (1)$$

where C_f^{∞} and C_s^{∞} are equilibrium concentrations of analyzed in the fiber and the sample matrix.

Distribution coefficient K_{fs} involves the distribution ratio of the concentration of analytes between the fiber coating sample matrix [73,74]:

$$K_{fs} = \frac{C_f}{C_s} \quad (2)$$

By converting the equations (1) and (2), another combination is obtained:

$$C_f^{\infty} = C_0 \frac{K_{fs} V_s}{K_{fs} V_f + V_s} \quad (3)$$

Then, the amount of analytes absorbed by the fiber coating is calculated using the equation below, which emphasizes that the amount of extracted analyte is directly proportional to its concentration in the sample:

$$n = C_f^{\infty} V_f = C_0 \frac{K_{fs} V_s V_f}{K_{fs} V_f + V_s} \quad (4)$$

The equation above can be simplified into a new one, if the volume of the sample is considerably large, i.e. $V_s \gg K_{fs}V_f$:

$$n = K_{fs}V_f C_0 \tag{5}$$

The equation (5) signifies that the method is useful even though the sample volume is unknown. This means that the fiber coating can be exposed into the flowing blood, ambient air, flowing water, etc. The amount of extracted analyte will be dependent and linearly correlate with its concentration in the sample, but not with the sample volume [74].

The thermodynamics of SPME process is described by distribution constant, i.e. distribution between the sample and the extraction phase. Distribution constant is presented as follows if the extraction medium is a liquid:

$$K_{es} = \frac{a_e}{a_s} = \frac{C_e}{C_s} \tag{6}$$

where a_e and a_s are the analyte's activities in the extraction phase and sample, approximated by its concentrations in these two different phases [75].

Moreover, the mass of extracted analytes is dependent on the total equilibrium of three phases (fiber, headspace, and sample) of the system. Since the amount of an analyte should be the same during the process, we obtain the following:

$$C_0V_s = C_f^{\infty}V_f + C_h^{\infty}V_h + C_s^{\infty}V_s \tag{7}$$

where C_0 is the initial concentration of analytes in the sample, C_f^{∞}, $C_h^{\infty}, C_s^{\infty}$are the equilibrium concentrations the fiber coating, the headspace and the sample, respectively. Volumes of the fiber, the headspace and the sample are denoted: V_f, V_h, V_s.

The mass of an analytes can be expressed as in the equation (8), when fiber/headspace distribution constant is defined as $K_{fh} = C_f^{\infty}/C_h^{\infty}$ and the distribution constant of headspace/sample is expressed as $K_{hs} = C_h^{\infty}/C_s^{\infty}$:

$$n = \frac{K_{fh}K_{hs}K_f C_0 V_s}{K_{fh}K_{hs}V_f + K_{hs}V_h + V_s} \tag{8}$$

The equation (8) can be rewritten as follows:

$$n = \frac{K_{fs}V_f C_0 V_s}{K_{fs}V_f + K_{hs}V_h + V_s} \tag{9}$$

The expression above emphasizes that the fiber's position in the system (in the

headspace or directly immersed in the sample) does not affect the amount of extracted analytes, if the volumes of the fiber, sample and headspace are kept constant [75, p.138]. Besides, for the determination of compounds with high volatility, location of the fiber in the headspace is more efficient and convenient than in the directly immersed position [76].

To quantify analytes in SPME sampling, different types of calibration methods can be used: external standard, internal standard and standard addition calibration. All these methods have their own conveniences, as well as drawbacks [77].

Compared to liquid extraction techniques, where all analytes from the matrix are extracted into the organic phase but only a small fraction (1/100 or 1/1000) is transferred to the analytical instrument, during SPME a small fraction of analytes is extracted into the fiber, instead all extracted analytes are desorbed in the analytical instrument [33]. Subsequently, exhaustive amount of analytes is not transferred to the extraction phase [34]. Furthermore, the method reduces use of organic solvents, complying with the 12 principles of green analytical chemistry and diminishes double contamination of the environment [35]. SPME has been used for a variety of applications: environmental, food, biochemical analysis, etc. [36–38]. Especially, the method is globally recognized and widely used in the analysis of different environmental objects: soil, water, air. SPME in couple with GC-MS is a promising technique for the determination of various classes of volatile and semi-volatile organic pollutants [39]. There are three different SPME extraction modes: direct extraction, extraction from a headspace and with a membrane protection. During direct mode the fiber is immersed into the sample with target analytes, and they are directly absorbed by the coating. To facilitate the extraction process certain agitation is necessary, depending on the sample [40,41]. Headspace mode involves extraction from the gaseous phase, for which analytes must be released from the sample bulk and overcome air resistance. Headspace mode helps to prevent the fiber coating from damages caused by the sample and overcomes interferences of other non-volatile undesirable compounds [42]. SPME with membrane protection adds an additional protection for the coating and is more useful in extraction of analytes with low volatilities. Also, the membrane provides some levels of selectivity to the process [43]. However, there is no significant difference between direct and headspace extraction modes, if analyzed sample volumes are the same. Besides, a quite difference undoubtedly occurs in the case of extraction of compounds with high volatility. Compared to direct mode, HSSPME shows better results and lower detection limits in the analysis of volatile organic compounds [44]. The developed SPME headspace mode is simple, time-efficient, affordable and provides low detection limits and easy automation in the analysis of VOCs [45]. Moreover, the volatility of the sample enhances the extraction efficiency of SPME. Recent studies utilizing SPME for BTEX analysis, as summarized in Table 3, have considered various analytical parameters. The choice of fiber coating significantly influences the performance of SPME methods. Generally, commercial

carboxen/PDMS, DVB/PDMS, and DVB/CAR/PDMS are the most commonly used SPME fiber coatings. For instance, Crom et al. [46] utilized CAR/PDMS fiber coatings in an SPME method for water samples to analyze BTEX. Optimal experimental parameters, including a sampling time of 60 minutes, adsorption temperature of 50 °C, and a 1:5 ratio of HS/sample volume, were determined to establish suitable sampling conditions. This method achieved a satisfactory recovery range of 70-125%. The extraction efficiency and mass transfer rate primarily depend on the adsorbent type, and the development of novel and efficient coating materials will further advance SPME. Table 3 highlights various materials with excellent adsorption capabilities, such as KAPs-triPB [47], PoA/GONSs [48], and PEG-g-MWCNTs [49], which have been utilized as SPME adsorbents for BTEX applications. Hosseinzadeh et al. [50] employed an ion pair of cationic surfactants (cetyltrimethylammonium bromide and tungestosilicic acid) incorporated in a PVC matrix as a highly sensitive SPME fiber for BTEX extraction from water. Different coating compositions were compared, and the 70:30 composition exhibited the highest extraction efficiency. Additionally, satisfactory relative standard deviations (RSD) ranging from 1.48 to 4.27% were achieved following optimization. Sarafraz-Yazdi et al. [51] developed a novel polypyrrole-carbon nanotubes-silicon dioxide (PPy-CNT-SiO2) SPME fiber for the preconcentration of BTEX in water. The inclusion of ultrafine SiO2 nanoparticles as colloidal substrates for conducting polymers (CPs) led to enhanced porosity and surface areas compared to PPy-CNT coating alone. The PPy-CNT-SiO2 fiber demonstrated excellent performance with low limits of detection (0.005-0.020 ng mL^{-1}), a wide linear range (0.01-200 ng mL^{-1}), and improved performance compared to other SPME adsorbents. The method exhibited an RSD of 3.9-8.5%, with relative recoveries ranging from 91.0 to 106.7% following optimization.

SPME is the most suitable and convenient method for the determination of organic pollutants in different matrices. A fast operation that does not require additional complex and expensive extraction components, automation of sample preparation in one single step makes SPME an indispensable method for fast and accurate analysis [60]. Furthermore, reduction of organic solvents application by SPME complies the technique with principles of green analytical chemistry [61]. Different modes of SPME were used for analysis of VOCs and other chemicals in various environmental samples [62]. SPME methods were optimized for the determination of BTEX in a range of sample matrices, as well as air, water, soil [63–65].

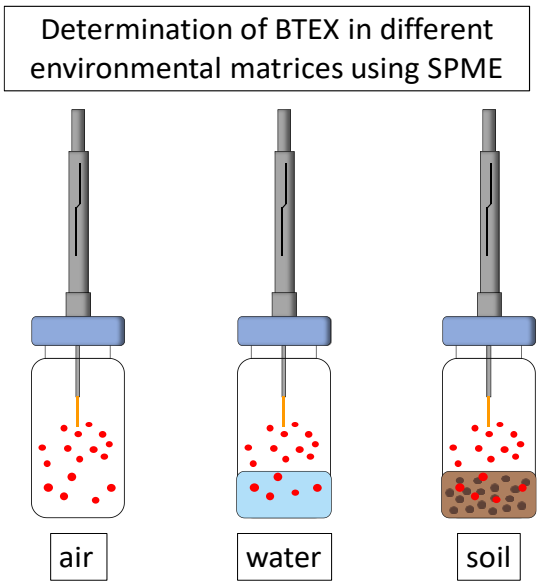


Figure 2 – Scheme of sampling of air, water and soil for SPME of BTEX

1.4 Optimization of SPME parameters

The optimization of SPME parameters stands as a crucial step in method development, typically employing a practical 'trial-and-error' approach in experimental design. The commonly optimized parameters are extraction temperature, fiber coating type, pressure in a vial, salting, pH, extraction time, organic solvent content, extraction time. Temperature in fiber has been studied recently by the PhD Orazbayeva's group.

Different types of coating are varied in use for SPME, the main parameters to distinguish is porous and non-porous coating. Porosity is effect on adsorption of analytes, which is considered as one of the main factors of extraction and fiber selected according to the suitability for the analyte nature.

In the case of temperature effect on distribution constant, the equation can be expressed as follows, if temperature values of the sample and fiber change from T_0 to T:

$$K_{fs} = K_0 exp\left[-\frac{\Delta H}{R}\left(\frac{1}{T}-\frac{1}{T_0}\right)\right] \quad (10)$$

where K_0 is the distribution constant between the fiber and sample at temperature T_0, K_{fs} is the distribution constant at temperature T, ΔH is the analytes' molar change in enthalpy releasing from the sample matrix and absorbing into the fiber coating and R is the universal gas constant [75, p. 275-278]. According to equation 10 it is understandable that distribution constant is inversely proportional to the temperature. Thus, increase in temperature will decrease distribution constant's value, even though high temperatures improve mass transfer of analytes and increase the extraction rate [78].

Temperature has an important influence on the SPME kinetics, due to the effect on

vapor pressure of analytes. It possesses two counterpart effects on the extraction process at the same time. Diffusion of analytes can be improved under elevating temperatures. It helps to transfer the analyzing compounds to the gaseous phase from the sample during the HSSPME [79]. Furthermore, high temperatures extend the application of HSSPME for the release to the headspace of semi-volatiles and compounds strongly bounded to the matrix sample. They reduce the fiber's longevity and cause a bleeding of the polymer coating [80]. As an example, in the analysis of BTEX in foundry molding sand, peak areas of analytes at 50 °C showed the highest responses, while at 25°C and 75°C small decreases were observed. Reversibly, the extraction of BTEX at 100 °C presented the lowest responses, which can be explained by poor diffusion of analytes onto the SPME fiber coating at elevated temperatures [81].

Furthermore, to overcome the drawbacks of SPME at elevated temperature values an internally cooled solid phase microextraction device was facilitated by Zhouyao Zhang and Januaz Pawliszyn in 1995. The main principle of the cold-fiber solid-phase microextraction (CF-SPME) method is to cool the SPME fiber coating, while simultaneously heating the sample matrix. With the cooled fiber coating it is easier for the fiber to absorb the analytes even at elevated temperatures, correspondingly enhancing the sensitivity of the analysis, without reducing the distribution constant. Using the equation below partition coefficient K_T of analytes between two phases at different temperatures can be calculated [73]:

$$K_T = K_0 \frac{T_s}{T_f} exp\left[\frac{C_p}{R}\left(\frac{\Delta T}{T_f} + \ln\frac{T_f}{T_s}\right)\right] \tag{11}$$

where $\Delta T = T_s - T_f$; K_0 is the distribution coefficient between the fiber coating and headspace when both are at temperature T_f. From equation (14) it can be stated that the lower the fiber coating's temperature, the larger the distribution coefficient. However, in practice there are limitations of the equation (14): decreasing the fiber's temperature to very low values affect the coating's physical and chemical properties, diminishes its extraction power and extraction rate can be decreased [73].

Another two parameters that improve the extraction from aqueous samples are salting out and adjusting of pH. Salting out can either increase or decrease the extraction based on the amount of added salt and its concentration. Addition of salt with concentration values more than 1% results in considerable improvement of extraction. Saturation of the sample matrix with salt also decreases sample's pH value, making it more acidic, due to the increase in activities of protons. Currently, there are no theoretical examinations of salting effect on SPME, nevertheless, there is a theoretical expression of its effect on liquid-liquid extraction. According to Setchenow's equation:

$$K_{fs} = K_0 e^{k_s C_s} = K_0 \left[1 + k_s C_s + \frac{(k_s C_s)^2}{2!} + \frac{(k_s C_s)^3}{3!} + \cdots\right] \quad (12)$$

where K_0 is the partition without salt, k_s is a constant and C_s is the concentration of added salt [73].

Pressure in the system is another significant factor affecting the extraction process. The extraction by the fiber coating of analytes under the reduced pressure conditions is called vacuum assisted headspace solid-phase microextraction, a method which was introduced by Brunton et al. for the first time. Elevated temperatures in the system result in higher pressure in the sample vial. This leads to decreased partition between the headspace and the liquid, which causes lower extraction by the SPME fiber and poor responses of target analytes [82]. According to estimated theory statements, partition coefficient between the gas and sample K_g is proportional to the analytes' molecular diffusion coefficient D_g raised to power m, which mostly equals to 0,5, 2/3 and 1:

$$k_g \propto D_g^m \quad (13)$$

Moreover, diffusivity correlations of binary gaseous mixtures at reduced pressure values ca be expressed by Fuller – Schettler – Giddings method. The Fuller – Schettler – Giddings method is one of the most precise approaches describing the correlation for nonpolar organic gases:

$$D_g = \frac{0.001 \times T^{1.75} \sqrt{(1/M_{air}) + (1/M_c)}}{P\left[(\sum V_{air})^{1/3} + (\sum V_c)^{1/3}\right]^2} \quad (14)$$

where T is the absolute temperature, M_{air} is the air's molecular weight, M_c is the organic compound's molecular weight, and V_{air} and V_c are the molar volumes of air and the organic compound of interest, respectively. The equation (14) shows that compound's molecular diffusion coefficient (D_g) is inversely proportional to the total pressure (P). Thus, decreasing the total pressure in the system increases the analytes' molecular diffusion coefficient, hence, the analytes' mass transfer and extraction rate increases [83]. HSSPME with reduced system pressure (Vac-HSSPME) has been successfully applied for the determination of various volatile and semi-volatile organic pollutants in different environmental samples [84,85]. The use of vacuum is beneficial for both porous and non-porous coating, but for porous coatings especially by reducing pore pressure and enhancing the effective diffusion coefficient of an analyte within them. This, in turn, accelerates the mass transport of analytes in porous coatings, potentially resulting in elevated extraction rates. Reduced pressure in the system of SPME vial can be easily achieved by air evacuation using the vacuum pump [82]. In addition, the set up for Vac-HSSPME is affordable,

convenient and very simple [86].

1.5 Modelling of SPME

1.5.1 COMSOL Multiphysics® for SPME simulation

Optimization of parameters for SPME, performing practical experimental studies, and evaluating and processing experiment results are time-, resource- and labor-consuming. Lately, it was proposed to optimize SPME parameters using mathematical [87,88] and computer modeling [89–94]. Hence, modeling of SPME and evaluation of parameters' effect on the extraction process using finite element analysis software, COMSOL Multiphysics ® has received attention in recent years for its rapid operation and fast outcomes attainment, compared to performing numerous expensive experiments. The computer simulation conducted using COMSOL Multiphysics® software was first proposed by the group of SPME developer Prof. Pawliszyn from University of Waterloo (Canada). In Prof. Pawliszyn's study the deep focus has been on computational-based model of extraction processes in SPME. Few factors were investigated with the model, i.e. effect of fiber's thickness, agitation of the sample and binding matrix components. The proposed model considered such processes as the fluid flow past the fiber coating, release of analytes from the sample to the fiber and mass transport from the coating, and absorption of target analytes by the fiber. Equations describing the fluid flow, time-dependent mass transport of analytes in the fiber and binding matrix component (humic organic matter) were applied for the model. The system has been validated through experimental study of the extraction of benzene from an aqueous samples using a PDMS fiber coating, performed by the research group more previously. The results showed that the generated model can predict the time when equilibrium is achieved with the presence of stirring of the sample or its absence. However, the model does not provide with the reassuring results related to the mass of extracted analytes during the absence of stirring. Besides, the simulated outcomes evaluating the thickness of the fiber coatings reliably correlated with the experimental results. It was determined that the shorter equilibration time is achieved if the ratio of analytes to binding matrix components is lower (1:100). A model that predicts the kinetics in SPME process during the extraction of analytes from the sample containing binding matrix compounds and matrix-free sample was proposed in the overall study. The proposed model and simulation can be employed to choose a suitable SPME fiber coating and predict the matrix effect on uptake kinetics, however, the majority of the work was focused on static conditions, since at each moment of time the amount of extracted analytes is higher due to the convection caused by the sample's movement [95].

In another study of Prof. Pawliszyn's research group the SPME geometries' effect on kinetics of extraction and its effectiveness were studied. It was confirmed that the mass flux is dependent on the fiber coating's size. Using the fiber with a smaller radius will result in

a shorter equilibration time and spherical shape was concluded to be preferable than cylindrical or planar shapes. The simulated model showed that higher sample depletion by the analytes leads to shorter equilibration times and with the smaller particles size the equilibration time is achieved much faster. Overall results of the model emphasizes that addition of large amount of particles does not always enhance the extraction and improve sensitivity, but might diminish the efficiency of the process[96].

In a work of Md. Nazmul Alam, Luis Alberto Ricardez-Sandoval, and Janusz Pawliszyn, applying COMSOL Multiphysics ® software diffusive sampling, when a fiber coating is immersed in a sample for a considerably short time, was considered, while diffusion boundary of molecules around the extractant, exposed to a sample, controls the extraction rate. During the study mathematical models and computational simulations were used, which could predict the main parameters for SPME with the diffusive sampling. The work also involved the dynamic conditions aspect, since the method described above requires an active stream of flowing analytes. The model, based on the extraction of aromatic polycyclic hydrocarbons (PAHs), showed that *K* values of analytes affect the equilibration time. High *K* values (equivalent to log*P* values) result in longer times of equilibration. The amount of extracted analytes during the initial stage, which involved diffusion control, were similar, because the diffusion coefficients of four selected analytes are close to each other. The proposed mathematical model was validated using comparison with practical experimental results from rapid sampling of benzene in water. The mass uptake can be precisely identified using the simulation and with the help of mechanistic model, involving parameters of the model with physical quantities, the mass-transfer process was ideally described. Furthermore, the model showed that fiber's rotation is requirable during sampling to achieve the usage of both sides of the coating [97].

1.5.2 Physical and mathematical models of SPME

Physical model of SPME includes the consideration of extraction phases according to the extracted analyte from the sample type (air, water, soil). SPME of VOCs in air involves a diffusion of analytes from air sample to the headspace [75]. This is why the diffusion of analytes to the extractant is considered as a rate-limiting factor of the mass transfer, which increases the equilibration time (Fig.3) [98]. Before transferring onto the fiber, the VOCs penetrate through the air resistance[75]. In SPME sampling of air, air – fiber coating distribution constant is the one of the most affecting parameters on the extraction [99]. Fick's second law of diffusion has been used to model mass transport in the gas phase:

$$\frac{\partial c}{\partial t} = D\ \nabla^2 \mathrm{c} \qquad (15)$$

where: *c* is the analyte concentration, mol m^{-3}; *D* is the diffusion coefficient of analyte

in a corresponding gas, $m^2 s^{-1}$; t is time.

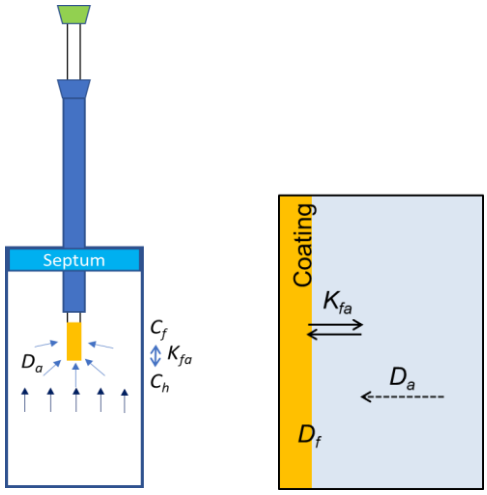


Figure 3 – Scheme of SPME of VOCs from air

Analysis of VOCs in water samples involves a release of analytes from the sample to the gaseous phase – headspace. Mass transfer from the water sample to the headspace is less challenging than from the soil, since there is no matrix effect, but distributed by the Henry's law constant. The process is described by sample – headspace and headspace – fiber distribution constants and analytes' diffusion coefficients (Fig.4) [75,99]. For water samples, liquid-phase diffusion coefficient is required to define solvent and solute liquid-phase mixture, where solute is considered as infinite diluted in the solvent. Wilke and Chang correlation for nonelectrolytes in infinitely dilute solution can describe the diffusion of analytes in water [100]:

$$D_w(\mathrm{m^2\ s^{-1}}) = 7.4 \cdot 10^{-8} \frac{(\varphi\, M(\mathrm{H_2O}))^{1/2} T}{\mu V_a^{0.6}} \qquad (16)$$

where φ is the association parameter of the solvent (2.26 for water), M (H_2O) is the molecular weight of water, μ is the dynamic viscosity of water (cP), V_a is the molar volume of an analyte at its normal boiling point (m^3 mol^{-1}).

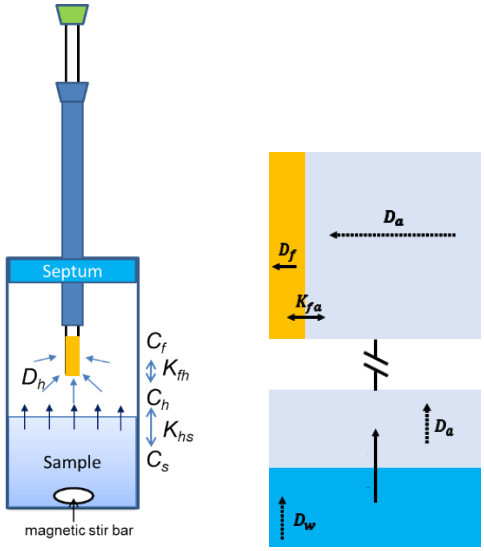


Figure 4 – Scheme of SPME of VOCs from water

Compared to sampling in air and water, diffusion of VOCs in soil is much slower. Analytes must be released from the strong matrix to the headspace. Then, by passing through the gaseous headspace resistance, the diffusion of them onto fiber surface is subsequent. As in water sampling, soil SPME sampling considers diffusion coefficients of analytes and headspace – sample and fiber – headspace distribution constants (Fig.5) [75,101].

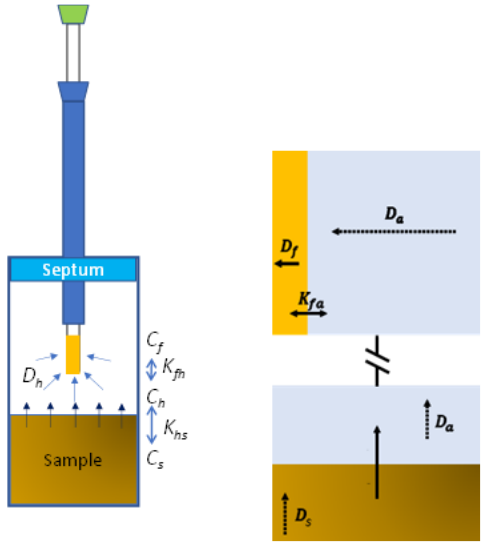


Figure 5 – Scheme of SPME of VOCs from soil

2 DEVELOPMENT OF COMPUTATIONAL MODEL FOR PREDICTING THE EFFECT OF TEMPERATURE ON SOLID-PHASE MICROEXTRACTION OF VOLATILE ORGANIC COMPOUNDS FROM AIR USING COMSOL MULTYPHYSICS

Preamble

The materials in this chapter have been partially published as research article: Anel Kapar, Aset Muratuly, Dina Orazbayeva, Nadezhda V. Bakaikina, Bauyrzhan Bukenov, Bulat Kenessov;* Modeling the effect of temperature on solid-phase microextraction of volatile organic compounds from air by polydimethylsiloxane coating using finite element analysis. *J.Anal Chim A.*, 2022, Vol. 1195. P. 339431. https://doi.org/10.1016/j.aca.2022.339431

2.1 Introduction

This research was aimed at developing a computational model for predicting the effect of temperature on extraction of VOCs from air onto SPME coating based on PDMS using CMP software. Development of such a model requires diffusion coefficients of analytes in air and fiber coating, as well as their distribution constants between a coating and air, which can be taken from the literature and estimated using existing theory or semi-empirical methods.

For predicting the diffusion coefficients of compounds in air, the semi-empirical methods proposed by Fuller et al. [102], Wilke and Lee [103], Hirschfelder et al. [104] were reported to provide the greater accuracy of prediction compared to other methods [105,106].

Herein, the molecular diffusion volumes are the additive values calculated by summarizing the atomic diffusion volumes. The atomic diffusion volumes are tabulated semi-empiric values reported by the authors [102].

The Hirschfelder et al. (Eq. 17) and Wilke and Lee (Eq. 18) methods introduce the collision integral (Ω_D), and Lennard-Jones collision diameter (σ_{AB}):

$$D_{AB} = \frac{0.008167T^{3/2}(\frac{1}{M_A}+\frac{1}{M_B})^{1/2}}{P\sigma_{AB}^2\Omega_D} \quad (17)$$

$$D_{AB} = \frac{[3.03-\left(\frac{0.98}{M_{AB}^{1/2}}\right)]10^{-3}T^{3/2}}{PM_{AB}^{1/2}\sigma_{AB}^2\Omega_D} \quad (18)$$

Herein, the collision integral Ω_D is calculated from the energy of molecular interaction and boiling point, and σ_{AB} is calculated from the specific volume of the saturated liquid at the boiling temperature [107].

The scarcity of experimental diffusion coefficients for VOCs in PDMS coating implies the need for use of predictive methods. The theory of diffusion of compounds in polymeric

systems is more complicated than in binary gas systems. Currently, the free-volume (FV) theory proposed by Vrentas and Duda is the most used theory for diffusion in polymeric systems [108]. For using predictive equation for the polymer/solvent binary mutual-diffusion coefficients using FV theory, the use of 13 independent descriptors and parameters is required [109]. These parameters are not available for a wide range of compounds. Different approximations were proposed in order to increase the predictive capability of the method and decrease the use of experimental data [108]. However, the method still is non-applicable for a wide range of compounds that were not covered in related research.

Inverse gas chromatography (IGC) has recently been re-discovered as a simple and straightforward method for experimental investigating of the properties of polymers [110]. In IGC, the polymer of interest is immobilized in the column as a stationary phase. Capillary columns, especially commercial ones, offer uniform thickness of the polymer coating, which decreases the scattering of the estimation results [110]. Most commercial nonpolar GC stationary phases are based on PDMS, which allows using them for estimation of PDMS sorption and diffusion parameters for various analytes. For estimating the diffusion coefficients of analytes in PDMS (D_s) using capillary IGC method, Golay equations [111] are commonly used:

$$H = \frac{B}{u} + (C_m + C_s)u \tag{19}$$

$$B = 2D_m \tag{20}$$

$$C_m = \frac{1+6k+11k^2}{24(k+1)^2}\frac{r^2}{D_m} \tag{21}$$

$$C_s = \frac{2k}{3(k+1)^2}\frac{d^2}{D_s} \tag{22}$$

where H is the theoretical plate height, B represents the longitudinal diffusion in mobile phase, C_m and C_s are the resistance to mass transfer in the mobile and stationary phases, respectively, u is the linear flow velocity, D_m is the diffusion coefficient in mobile phase, k is the retention factor, r is the internal radius of a column, d is the thickness of the stationary phase, D_s is the diffusion coefficient in the stationary phase.

PDMS coating was chosen for this study because distribution constants between this coating and air (K_{fa}) at different temperatures can be estimated using van 't Hoff equation [112]:

$$K_{fa} = K_{fa}^0 \exp\left[-\frac{\Delta H}{R}\left(\frac{1}{T} - \frac{1}{T_0}\right)\right] \tag{23}$$

where K_{fa}^0 is the distribution constant at temperature T_0 (K), ΔH is the molar heat of absorption of an analyte, and R is the gas constant.

The value of ΔH for volatile compounds distributed in PDMS can be approximated by the heat of vaporization of a pure compound ΔH_{vap} [112]. Coating-air distribution constants at T_0 (298 K) can be estimated using two approaches based on:

– linear temperature programmed retention indices (LTPRI) [113];

– linear solvation energy relationship (LSER) model for characterization of sorption interactions [114].

The LTPRI approach uses the linear relationship between logK_{fa} of compounds and their retention indices on a GC capillary column with identical composition. The relation for PDMS [113] is:

$$logK_{fa} = 0.00415\ LTPRI - 0.188 \quad (24)$$

where *LTPRI* is the retention index of a compound relative to the retention of *n*-alkanes on the identical stationary phase:

$$LTPRI = 100N + 100\left(\frac{t_{R(a)} - t_{R(N)}}{t_{R(N+1)} - t_{R(N)}}\right) \quad (25)$$

where N is the number of carbon atoms; $t_{R(a)}$ is the retention time of an analyte; $t_{R(N)}$ and $t_{R(N+1)}$ are the retention times of *n*-alkanes eluting before and after the analyte.

LSER uses the following equation by using PDMS coating[123]:

$$\log K_{fa} = \mathrm{c} + sS + aA + bB + l\ L \quad (26)$$

where *S* is the solute dipolarity/polarizability parameter, *A* is the measure of the solute hydrogen-bond acidity, *B* is a measure of the solute hydrogen-bond basicity, L is the solute gas–liquid distribution coefficient on *n*-hexadecane at 298K and represents dispersion/cavity interactions, *c*, *s*, *a*, *b* and *l* are multiple regression coefficients determined for PDMS by Prikryl and Sevcik [114] at different humidity of air.

In this study, most accurate and suitable methods for estimating the diffusion coefficients of benzene, toluene, ethylbenzene, o-xylene (BTEX) in air and PDMS coating, distribution constants of the analytes between the coating and air at different extraction temperatures were selected. BTEX compounds were chosen because they are major toxic environmental pollutants [115], for which a lot of valuable experimental information is available. The computational model developed using COMSOL Multiphysics® software and the chosen methods were applied for several important and complex cases involving extraction of BTEX.

2.2 Methods

2.2.1 General modeling parameters

Models were built in two dimensional (2D) assymetric three-dimensional (3D) space dimensions using ‘Transport of Diluted Species’ physics in a ‘time-dependent’ model. The geometry consisted of three domains: air in the vial or in the gas sampling bulb, fiber core, and fiber coating (2D geometry is shown in Fig.7, 3D geometry is shown in Fig. 6). The model included the temperature dependencies of the diffusion coefficients in the fiber coating (D_f) and air (D_a), and distribution coefficients between the coating and air (K_{fa}). At the model development stage, the extraction temperature and pressure were assumed

constant and homogeneous in all domains. The processes were simulated for all studied analytes simultaneously.

To model mass transport in air and coating, Fick's second law of diffusion was used. The list and values of parameters used for modeling is provided in tables 4-6.

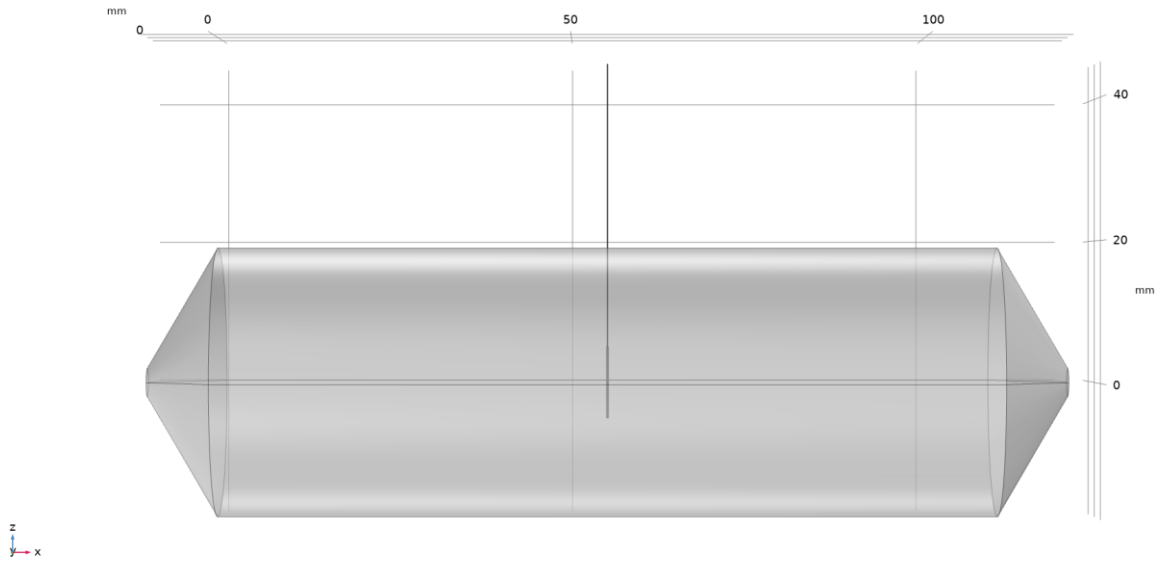


Figure 6 – 3D geometry of the SPME from 125 mL gas sampling bulb

‘Partition Condition’ feature was used to model the mass transport of an analyte between the coating and air. This feature assumes that the equilibrium on the boundary between two phases is established immediately and can be described by a partitioning coefficient (K_{fa}). In the previous studies, for such purpose, we used a more complicated approach based on calculating fluxes from air to coating and from coating to air and setting flux coefficients very high in order not to affect the extraction process [116].

Table 4 - General model parameters

Parameter	Value	Description
CoatTh	0.095 [mm]	Coathing thickness
CoreD	0.11 [mm]	Core diameter
FiberDepth	VialH-40[mm]	Fiber injection depth
VialV	20 [ml]	Vial volume
VialD	20 [mm]	Vial diameter
VialH	4*VialV/pi/VialD^2	Vial height
CoatL	1[cm]	Coating length
BulbD	38 [mm]	Bulb diameter
BulbH	4*(VialV-2*ConeVs)/pi/VialD^2	Bulb length
BulbV	125 [ml]	Bulb volume
ConeRs	2[mm]	Small cone base radius
ConeH	10[mm]	Cone height (w/o small cone)
ConeVf	pi*(VialD/2)^2*ConeHf/3	Cone volume (with small cone)
ConeHf	ConeH+ConeHs	Cone height (with small cone)
ConeV	ConeVf-ConeVs	Cone volume (w/o small cone)
ConeHs	ConeRs*ConeH/(VialD/2-ConeRs)	Small cone height
ConeVs	pi*ConeRs^2*ConeHs/3	Small cone volume
T	(TC+273.15) [K]	Experimental Temperature
p	0.9 [atm]	Pressure
C_0	250[ug/m^3]	Initial concentration in air
TC	30	Temperature in Celsius

Table 5 - Analyte parameters required for the model

Parameter	Description	Units
Mr	Molar mass	g/mol
Vi	Molar volume - LeBas	dimensionless
K0 (LTPRI)	LTPRI distribution constant value at T=298.15 K	dimensionless
K0 (LSER)	LTPRI distribution constant value at T=296.15 K	dimensionless
ΔH	Heat of vaporization	kJ/mol
df_slope	Slope of the lnD = f(1/T) plot	dimensionless
df_intercept	Intercept of the lnD = f(1/T) plot	dimensionless
S	Dipolarity/polarizability parameter	dimensionless
A	Hydrogen-bond acidity	dimensionless
B	Hydrogen-bond basicity	dimensionless
L	Gas–liquid distribution coefficient on *n*-hexadecane at 298K	dimensionless

Table 6 - Parameters of target analytes

Parameter	Benzene	Toluene	Ethylbenzene	*o*-Xylene
Mr	78.11	92.14	106.17	106.16
Vi	90.7	118.2	140.4	140.4
K0 (LTPRI)	296	815	2020	2710
K0 (LSER)	582	2078	5675	8721
dH	34.27	39.56	43.99	45.32
df_slope	-1926	-2271	-2847	-2744
df_intercept	-18.8	-17.5	-16.5	-16.9
S	0.51	0.520	0.51	0.56
A	0	0	0	0
B	0.13	0.14	0.15	0.16
L	2.786	3.325	3.778	3.937

‘Partition Condition’ feature was used to model the mass transport of an analyte between the coating and air. This feature assumes that the equilibrium on the boundary between two phases is established immediately and can be described by a partitioning coefficient (K_{fa}). In the previous studies, for such purpose, we used a more complicated

approach based on calculating fluxes from air to coating and from coating to air and setting flux coefficients very high in order not to affect the extraction process [116].

Simulations were conducted for 23-ga 100 µm PDMS fiber (Supelco, Bellefonte, PA, USA) with a fused silica core having a diameter of 110 µm and a length of 80 mm; the coating thickness and length were 0.095 and 10 mm, respectively [112]. The 'extra fine free triangular mesh' was used for the modeling. To provide better meshing at the coating-air interface, the resolution of narrow regions was increased to '10'. For time-weighted average (TWA) SPME, this parameter was set to 5. The parametric sweep was used to obtain the computational extraction profiles at different extraction temperatures. Surface (for 2D) or volume (for 3D) average concentrations in the coating were calculated and used for further data processing.

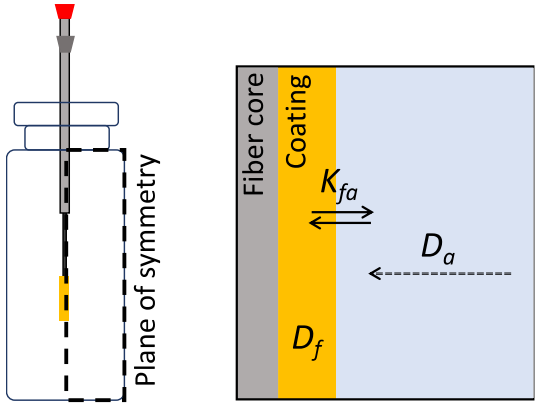


Figure 7 – Schematic representation of the SPME process in COMSOL Multiphysics® model (2D axisymmetric)

2.2.2 Estimation of coating-air distribution constant

Coating-air distribution constants at different temperatures were estimated using Eq. (23). Coating-air distribution constants for BTEX at 25 °C determined using LTPRI approach were taken from Pawliszyn [112]. For estimating coating-air distribution constants using LSER approach, Eq. (26) was used. Values of *S*, *A*, *B* and *L* were obtained from the UFZ-LSER database v3.2.1 [117]. Multiple regression coefficients *c*, *s*, *a*, *b* and *l* for PDMS coating were taken from Prikryl and Sevcik [114]. The values of ΔH_{vap} for analytes at 25 °C were taken from Majer et al. [118].

2.2.3 Estimation of diffusion coefficients in air

The methods of Fuller et al. [102], Wilke and Lee [103], Hirschfelder et al. [104], and Eqs. (14, 18,17), respectively, were used for estimating diffusion coefficients in air for BTEX. The results were compared with experimental values reported in the literature. The most accurate and efficient method was chosen, and its equation was added to the CMP model.

2.2.4 Estimation of diffusion coefficients in the PDMS coating

The temperature dependence of the infinite dilution diffusion coefficients of compounds in polymer is described by the Arrhenius equation:

$$D_{12}^{\infty} = D_0 \exp\left(-\frac{E_a}{RT}\right) \quad (27)$$

where D_0 is the pre-exponential factor for the analyte-polymer system, and E_a is the activation energy of diffusion.

Using values of D_f determined by capillary inverse gas chromatography and by Boscaini et al. [119] by a membrane-introduction proton-transfer reaction mass spectrometry (MI-PTRMS) approach, linear dependences of $\ln D_f$ on T^{-1} were obtained for each analyte and added to the CMP model.

2.3 Experimental

2.3.1 Reagents and materials

Benzene (99.9%), toluene (99.9%), ethylbenzene (99.8%), and o-xylene (97.0%) were purchased from Sigma-Aldrich (Germany). Methanol (HPLC grade) purchased from AppliChem (Germany) was used for the preparation of standard solutions of analytes. SPME was conducted using a 100 μm polydimethylsiloxane (PDMS, Supelco, USA) fiber coating from 125-mL gas sampling bulb (Supelco, USA) with cylindrical Thermogreen LB-1 septum (Supelco, USA).

2.3.2 Parameters of gas chromatography-mass spectrometry (GC-MS) analysis

For SPME experiments, the GC-MS analyses were performed on the 6890N/5973N system (Agilent, USA) equipped with flame ionization detector (FID), two split/splitless inlets and Combi-PAL (CTC Analytics, Switzerland) autosampler. Analytes were desorbed from the SPME fibers for 1 min at 250 °C in a GC inlet working in a splitless mode. Separation was conducted using a 30 m × 250 μm × 1.4 μm DB-VRX (Agilent, USA) column at the constant helium (>99.995%, Orenburg-Tehgas, Russia) flow 1.0 mL min^{-1}. The oven temperature was programmed from 40 °C (held for 5 min) to 75 °C (held for 0 min) at the heating rate 10 °C min^{-1}, then to 87 °C (held for 2 min) at the rate 3 °C min^{-1}, then to 120 °C (held for 0 min) at the rate 10 °C min^{-1}, and post run at 250 °C for 2 min. The temperatures of the MS ion source, quadrupole and interface were 230, 150 and 240 °C, respectively. Detection was conducted using the electron impact ionization at 70 eV in the selected ion monitoring (SIM) mode. The MS program used for the detection of the analytes in the SIM mode is provided in Table A4 in Supplementary material.

IGC experiments were conducted on the same instrument using the flame ionization detector. Separations were conducted on a 30 m × 0.25 mm (1.0 μm film) Rxi-1ms (100% PDMS, Restek, USA) column at 50, 75 and 100 cm s^{-1} helium (> 99.999%, Orenburg-Tehgas, Russia) flow. The detection was conducted at hydrogen flow 40 mL min^{-1}, air flow 450 mL min^{-1}, makeup flow (helium) 40 mL min^{-1}. The detector temperature was set to 250 °C. The gas phase (V = 5.0 μL) above the mixture of pure analyte (5.0 μL of each analyte) in 2 mL vial was injected using a gas tight syringe (Agilent, USA) into the GC inlet equipped with a 0.75 mm i.d. splitless liner (Supelco, USA) at 200 °C and 50:1 split. The isothermal chromatograms were obtained at 40, 50, 60 and 70 °C. The detector data rate was 10 Hz.

2.3.3 Determination of diffusion coefficients in PDMS using inverse gas chromatography

Diffusion coefficients were determined using Eqs. (14, 17, 18) and obtained chromatograms. Height of a theoretical plate was calculated for each peak using:

$$H = \frac{L\,\sigma^2}{t_R^2} \tag{28}$$

where L is the column length, t_R is a retention time of a peak, σ^2 is the peak variance (second moment). Retention times of peaks, times of start and end of each peak were calculated using Data Analysis feature in Agilent MSD ChemStation (ver. E.02.02) software. Data files were exported in .CSV format and processed in Excel (Microsoft, USA) software to determine a variance σ^2 of each peak using:

$$\sigma^2 = \frac{\sum y_i(x_i - t_r)^2}{\sum y_i} \tag{29}$$

where x_i is a time, y_i is a detector response at x_i, t_R is a retention time. Retention factors k was calculated using:

$$k = \frac{t_R - t_{R0}}{t_{R0}} \tag{30}$$

where t_{R0} is a void time that was calculated by dividing the column length by an average linear flow velocity (taken from MSD ChemStation software).

Diffusion coefficients of analytes in a mobile phase were determined by Fuller method [102] at the average pressure in the column using [120]:

$$p = \frac{p_o}{j} \tag{31}$$

where p_o is the atmospheric pressure in the laboratory (0.9 atm), j is the compressibility determined using:

$$j = \frac{3}{2}\left[\frac{(p_i/p_o)^2 - 1}{(p_i/p_o)^3 - 1}\right] \tag{32}$$

where p_i is the absolute pressure in the GC inlet (a sum of atmospheric pressure p_o and the gauge pressure according to MSD ChemStation software).

For benzene and toluene, mean diffusion coefficients in the stationary phase were calculated based on results obtained at average linear velocities 50, 75 and 100 cm s^{-1}, for ethylbenzene and o-xylene - at 75 and 100 cm s^{-1}.

2.3.4 Experimental study of the effect of the temperature on extraction profiles of analytes

SPME was conducted using a 100 μm PDMS fiber coating from the 125-mL gas sampling bulb. To avoid possible matrix effects, the bulb was filled with a laboratory air purified from water and BTEX. From one side, the bulb was connected to the air sampling pump Pocket Pump TOUCH (SKC Inc., USA) working at the rate of 100 mL min^{-1}. From another side, the bulb was connected to the U-shaped 5-mL sparger tube (Teledyne Tekmar, USA) filled with 4Å zeolite ("Promhim" LLC, Russia) and activated carbon AG-3 ("Sorbent" JSC, Russia) granules, and 40-mL bubbler (ID = 15 mm, height = 240 mm) cooled with ice. Before use, zeolite and activated carbon were cleaned in a drying cabinet at 150 °C during 3-5 h.

Gas standards of analytes were prepared from pure standards by serial dilution in 1000 mL and 125 mL gas sampling bulbs. Into 125-mL extraction bulb, 30.0 μL of gas standard was injected using gas tight syringe (Supelco, USA) to provide the 250 ng L^{-1} concentration of each analyte. The SPME was conducted at 25 and 40 °C for 5, 10, 20, 30, 45, 60, 90, 120 and 180 s. Extraction at T>25 °C was conducted in a temperature-controlled drying oven VAC-24 (Stegler, China). Before introducing the pre-conditioned (in the GC inlet at 250 °C) or removed after a previous desorption 100 μm PDMS fiber into the bulb, it was cooled to the extraction temperature during ~5 min in the 20-mL vial filled with a pure air. To purify the air in this vial, it was extracted three times (5 min each) by a pre-conditioned (in the GC inlet at 250 °C) 85 μm Carboxen/PDMS fiber. To remove water and other possible interferences, 4Å zeolite ("Promhim" LLC, Russia) and activated carbon AG-3 ("Sorbent" JSC, Russia) granules were introduced into the vial. The experiment was repeated three times. A relative extracted amount of an analyte (%) was calculated by dividing its peak area at an extraction time by its peak area at the equilibrium (mean for the last two or three points at the profile).

2.4 Results and discussion

2.4.1 Selection of the method for estimating diffusion coefficients in air

Percentage differences between predicted and experimental results were in the range from 0.5 to 7.2% with Fuller [102] equation, from 0.4 to 18.7% with Hirschfelder et al. [104] equation, and from 0.5 to 11.7% with Wilke and Lee [103] equation (Table 7).

Fuller method [102] was proposed based on the large dataset of measured diffusion coefficients for binary gas-phase systems, including VOCs-air, which resulted in a better accuracy of the method for organic compounds in air [106]. Compared to other methods for predicting the diffusion coefficients of binary gas-phase systems, the Fuller method allows obtaining diffusion coefficient values for various classes of compounds without additional experimental or predicted characteristics such as molar volume at critical boiling point, molar volume at normal boiling point, critical temperatures, etc. Since these values are not available for a large range of the compounds, the use of other estimating methods is rather limited. Therefore, Fuller method was selected as optimal for predicting the diffusion coefficients of compounds in air for this model.

Table 7 – Comparison of diffusion coefficients of BTEX in air ($cm^2\ s^{-1}$) obtained using predictive equations with experimentally measured values

T (°C)	Measured[a]	Estimated			Percentage difference between estimated and measured values[b]		
		Fuller	Hirschfelder	Wilke-Lee	Fuller	Hirschfelder	Wilke-Lee
Benzene-Air binary system							
25	0.0932	0.0894	0.08682	0.0936	4.1	-6.8	0.5
25	0.0849 [121]	0.0894	0.08682	0.0936	5.3	2.3	10.3
25.2	0.0962 [102]	0.0895	0.08693	0.0938	-6.9	-9.6	-2.5
35	0.1021 [102]	0.0947	0.09243	0.0997	-7.2	-9.5	-2.3
40	0.0957 [121]	0.0974	0.09529	0.1028	1.8	-0.4	7.4
Toluene-Air binary system							
25	0.0849 [122]	0.0804	0.0769	0.0825	-5.3	-9.5	-2.8
33	0.0876 [122]	0.0842	0.0808	0.0868	-3.9	-7.7	-0.9
25	0.0849 [105]	0.0804	0.0769	0.0825	-5.3	-9.5	-2.8
30	0.0880 [123]	0.0827	0.0793	0.0852	-6.0	-9.8	-3.2
40	0.0819 [121]	0.0876	0.0844	0.0907	6.9	3.0	10.7
Ethylbenzene-Air binary system							
25	0.0755 [105]	0.0735	0.0696	0.0745	-2.6	-7.8	-1.3
o-Xylene-Air binary system							
25	0.0727 [105]	0.0735	0.0697	n/a	1.2	-4.2	n/a

Notes: [a] Measured values were obtained from previous studies

[b] Percentage differences were calculated using the formula: $\frac{D_{measured}-D_{estimated}}{D_{measured}} . 100\%$

n/a – not available.

2.4.2 Diffusion coefficients in the PDMS coating

Diffusion of analytes in the coating can have a substantial effect on extraction profiles of analytes from air [124]. At lower K_{fa}, this effect is more pronounced because the equilibration is faster (lower amount of an analyte must be extracted to reach the equilibrium) and diffusion in the coating becomes a limiting stage in the extraction process (Fig. 8). At K_{fa} = 1000 and $D_f = 2 \cdot 10^{-9}$ m^2 s^{-1}, 80% of the equilibrium amount is extracted in 6.5 s. The decrease of D_f to 10^{-11} m^2 s^{-1} results in the 5-fold increase in this time (to 32.6 s). At K_{fa} = 10,000, similar decrease in D_f results only in the 43% increase in this time (from 46 to 66 s).

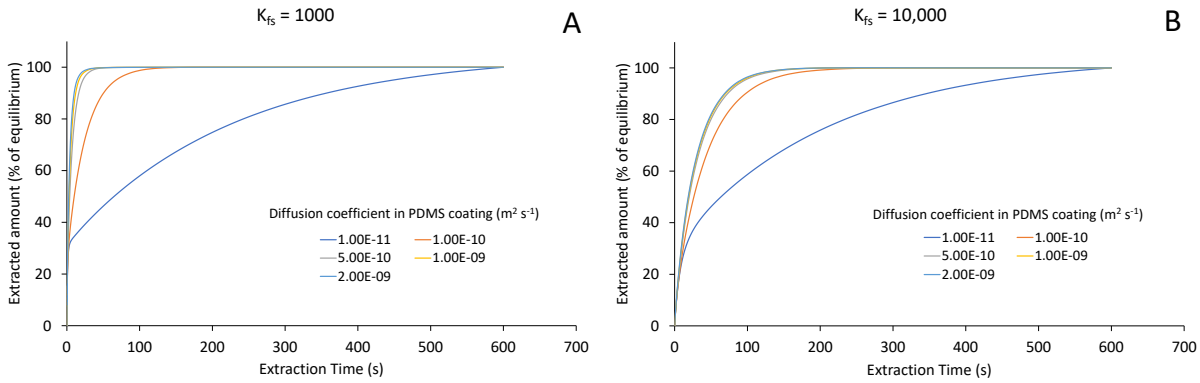


Figure 8 – Effect of the diffusion coefficient in PDMS coating on extraction profile of an analyte with a fiber-air distribution constant 1000 (A) or 10,000 (B).

In this study, capillary inverse gas chromatography on a column coated with 100% PDMS stationary phase was chosen for estimating diffusion coefficients of analytes in PDMS coating at different temperatures. Obtained '$\ln D_f$ = f (T^{-1})' plots were linear with R^2 = 0.92 for toluene and 0.98-0.99 for other analytes (Fig. 9) and allowed obtaining equations for their implementation into CMP model. Diffusion coefficients calculated using these equations at 25-70 °C were 1.9-2.5, 1.8-2.9, 1.7-1.3 and 1.2-1.3 times higher than using the equations obtained on the data reported by Boscaini et al. [119] (Table 8) for benzene, toluene, ethylbenzene and o-xylene, respectively. Diffusion coefficients for benzene and toluene at 25 °C are 2.7 and 4.8 times higher, respectively, than those reported by Chao et al. [125] for 100 µm PDMS fiber (1.01×10^{-10} m^2 s^{-1} and 0.44×10^{-10} m^2 s^{-1}, respectively).

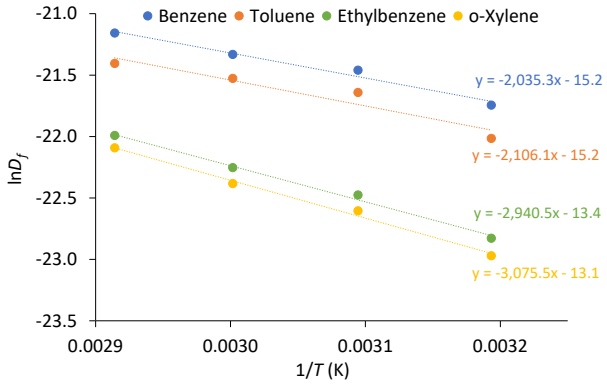


Figure 9 – Dependences of lnD_f on T^{-1} obtained using inverse gas chromatography

Table 8 – values of D_p measures by MI-PTRMS and IGC methods at different temperatures

T		Benzene	Toluene	Ethylbenzene	O-Xylene
30 °C	MI-PTRMS×10^{-10}	1.55	1.27	5.70	6.51
	IGC×10^{-11}	2.70	0.96	0.53	0.39
40 °C	MI-PTRMS×10^{-10}	1.81	1.40	8.20	8.82
	IGC×10^{-11}	2.34	1.80	0.81	0.65
50°C	MI-PTRMS×10^{-10}	2.80	1.55	1.15	1.17
	IGC×10^{-11}	2.10	2.60	1.07	1.05
60 °C	MI-PTRMS×10^{-10}	2.37	1.69	1.59	1.54
	IGC×10^{-11}	2.06	2.70	1.24	1.09
70 °C	MI-PTRMS×10^{-10}	2.69	1.84	2.15	1.98
	IGC×10^{-11}	2.44	1.90	1.34	1.25

2.4.3 Selection of the approaches for predicting PDMS-air distribution constants and diffusion coefficients in PDMS coating

Lowest values of root-mean-square deviation (RMSD) from experimental extraction profiles of benzene (5.4%) and toluene (5.1%) from 125 mL gas sampling bulb at 25 °C were obtained using D_f values determined by IGC and K_{fa} values estimated by LSER (Figs. 10A-D, Table 9). Similar values were obtained using IGC and LTPRI – 5.8% for benzene and 5.4% for toluene and using MI-PTRMS and LTPRI – 6.4% for benzene and 5.3% for toluene. Lowest RMSD values for ethylbenzene (10.6%) and o-xylene (13.3%) at 25 °C were obtained using the combination of IGC and LTPRI approaches. For ethylbenzene and o-xylene, RMSD values can be decreased to <5% by increasing their D_f values over those obtained by IGC by 2 and 3 times, respectively.

At 40 °C (Figs. 10E-H), MI-PTRMS in combination with LTPRI provided lowest RMSD values for benzene (5.4%) and toluene (4.5%). For these analytes, RMSD values were below 10% using all approaches, which can be caused by a low K_{fa} value of benzene and its quick equilibration between coating and air (Fig. 8). For ethylbenzene (5.2%) and o-xylene (4.5%), lowest RMSD values were obtained using IGC+LTPRI. Using other approaches, RMSD values were >10%, except MI-PTRMS+LTPRI for o-xylene (6.6%).

A combination of IGC and LTPRI was chosen for modeling purposes because in most cases it provided lowest RMSDs from experimental extraction profiles or they were below 10%. Greater RMSD values observed for ethylbenzene and o-xylene at 25 °C can be caused by the difference in the PDMS structure (e.g., crosslinking degree that can substantially vary for different synthesized PDMS affecting on the different number of possible configurations of the lattice, that ultimately unfavors adsorbtion in the polymer matrix. [126]) of the 100 μm SPME coating and the stationary phase in Rxi-1ms column.

Table 9 – RMSD values at different combinations of D_f and K_{fa} used for predicting extraction

D_f			K_{fa}			RMSD	
Method	Value, m^2s^{-1}		Method	Value			
	25 °C	40 °C		25 °C	40 °C	25 °C	40 °C
Benzene							
MI-PTRMS	1.4×10^{-10}	1.8×10^{-10}	LTPRI	296	153	6.4	5.4
			LSER	582	300	7.9	6.0
IGC	2.7×10^{-10}	3.7×10^{-10}	LTPRI	296	153	5.8	9.1
			LSER	582	300	5.4	8.2
Toluene							
MI-PTRMS	1.2×10^{-10}	1.4×10^{-10}	LTPRI	815	380	5.3	5.6
			LSER	1866	869	10.2	8.2
IGC	2.1×10^{-10}	2.9×10^{-10}	LTPRI	815	380	5.4	8.0
			LSER	1866	869	5.1	5.7
Ethylbenzene							
MI-PTRMS	4.7×10^{-11}	8.2×10^{-11}	LTPRI	2020	863	18.2	11.5
			LSER	5034	2152	25.4	16.6
IGC	7.8×10^{-11}	1.3×10^{-10}	LTPRI	2020	863	10.6	5.2
			LSER	5034	2152	11.5	11.0
IGC(x2)	1.6×10^{-10}	n/r	LTPRI	2020	n/r	3.8	n/r
o-Xylene							
MI-PTRMS	5.6×10^{-11}	8.9×10^{-11}	LTPRI	2710	1129	15.6	6.6
			LSER	7707	3211	26.5	13.8
IGC	6.6×10^{-11}	1.1×10^{-10}	LTPRI	2710	1129	13.3	4.5
			LSER	7707	3211	15.7	11.4
IGC(x3)	2.0×10^{-10}	n/r	LTPRI	2710	n/r	4.4	n/r

Note: n/r- not required

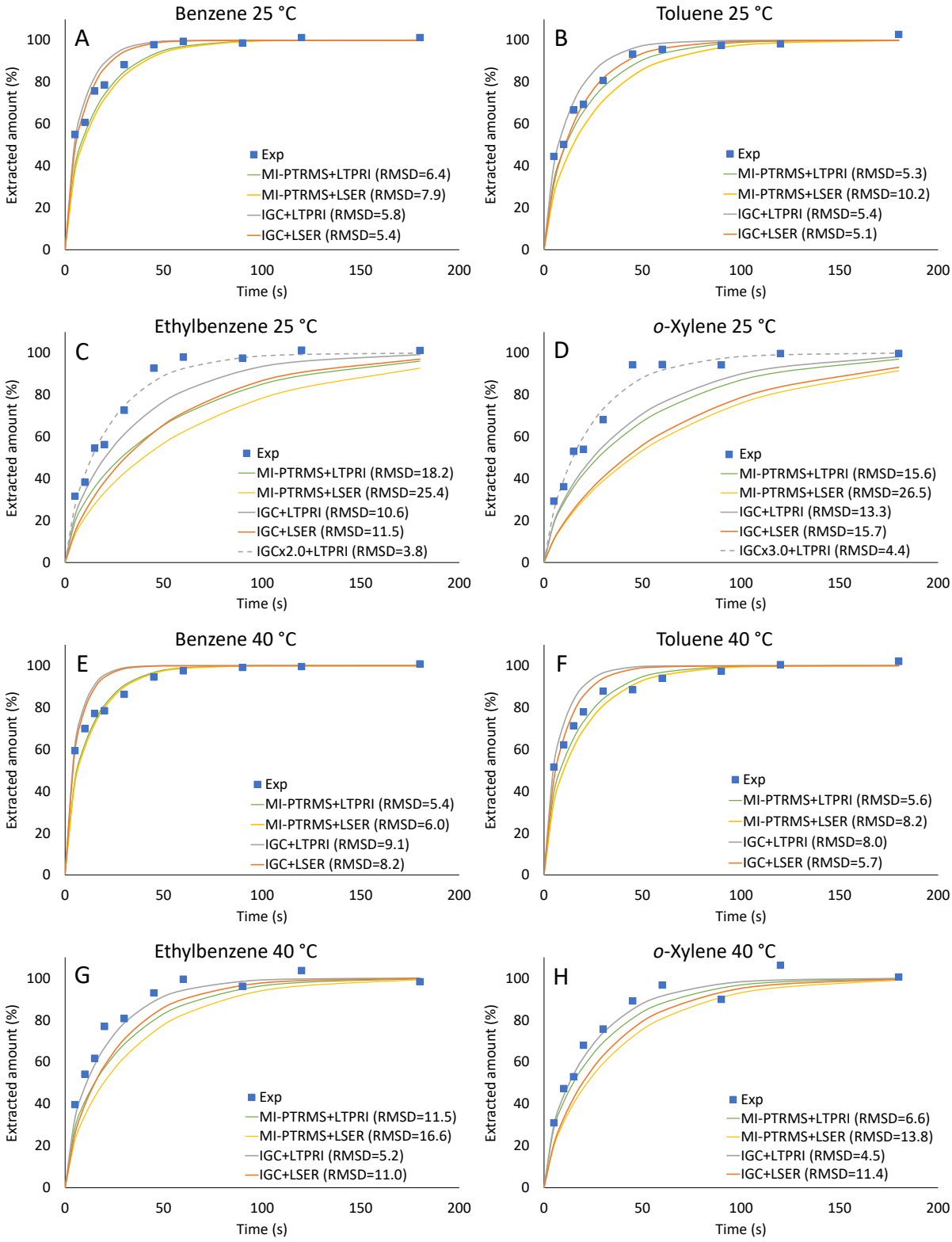


Figure 10 – Comparison of experimental profiles of BTEX sampling by a 100 µm PDMS fiber from 125 mL air sample (C = 250 µg m^{-3}) at 25 and 40 ºC with profiles obtained using CMP with different models for estimation of K_{fa} and D_f.

2.6 Chapter conclusion

Thus, a new COMSOL Multiphysics® based computational model for predicting the effect of temperature on extraction of VOCs from air onto SPME coating based on PDMS has been developed using existing theory and models. Fuller method was chosen for calculating diffusion coefficients of analytes in air due to its simplicity and reliability. Fiber-air distribution constants at different temperatures were estimated using van't Hoff equation. A combination of capillary inverse gas chromatography using a 0.25 mm column with 1 μm layer of 100% PDMS for determination of diffusion coefficients of analytes in the fiber and LTPRI for estimating distribution constants at initial temperature was chosen for modeling because in most cases it provided lowest RMSDs from experimental extraction profiles or they were below 10%.

The model was applied for obtaining temperature dependences of the extracted amounts of BTEX from 20-mL vials filled with air and from open air at different extraction times. It was also applied for obtaining extraction profiles by exposed and retracted fiber from open air at varying temperatures during extraction. The developed model can be used for obtaining simulated extraction profiles at different temperatures, pressures, sample volumes and geometries at constant or changing conditions. Its main advantage is the possibility to quickly optimize extraction time at any chosen conditions. Almost all input data can be found in scientific literature and databases or predicted using approaches reported in this manuscript. The only experimental step that should be done by end-users of the developed model is the determination of diffusion coefficients in the fiber using inverse gas chromatography (if they are not reported in the literature). However, this step is much simpler and faster than obtaining extraction profiles of analytes at different temperatures and other extraction conditions.

In the future, a database of D_f values in PDMS can be created. The developed model can be improved by modeling the matrix effects (humidity and other VOCs). It can also be expanded to porous fibers, liquid and solid samples. For porous fibers, a model to estimate the effect of temperature on fiber-air distribution constant will be required. For liquid samples, it will be necessary to model the effect of pH, ionic strength, temperature and agitation on Henry's law constant and mass transport of analytes. For solid samples, the effects of temperature and moisture content on a headspace-sample distribution constant and mass transport of analytes should be modeled.

3 MODELING HEADSPACE SOLID-PHASE MICROEXTRACTION OF VOLATILE ORGANIC COMPOUNDS FROM WATER SAMPLES WITH POROUS COATINGS USING FINITE ELEMENT ANALYSIS

The materials in this chapter have been published as research article: A. Muratuly, A. Kapar, B. Kenessov, Modeling headspace solid-phase microextraction of volatile organic compounds from water samples with porous coatings using finite element analysis, *J.Advances in Sample Prep.*, 2022. Vol. 3 https://doi.org/10.1016/j.sampre.2022.100030

3.1 Introduction

This research is aimed at the development of a more advanced CMP model for simulating the HSSPME of VOCs from water using 85 µm Car/PDMS coating. Compared to existing models, it should take into consideration the mass transport of an analyte in the aqueous phase and at the headspace-water boundary. It should also include functions for predicting coating-air and air-water distribution constants at different extraction parameters. Knowledge gaps and future directions in the development of this research area are discussed.

3.2 Theory

In HSSPME, three phases are involved – water, headspace and fiber coating. To model this process without agitation, diffusion coefficients in water, headspace and coating, coating-headspace and headspace-water distribution constants are required (Fig. 11a). When agitation is present, a more complicated model is required involving laminar or turbulent flow in water (Fig. 11b). In this case, mass transport at the boundary layer is controlled by diffusion.

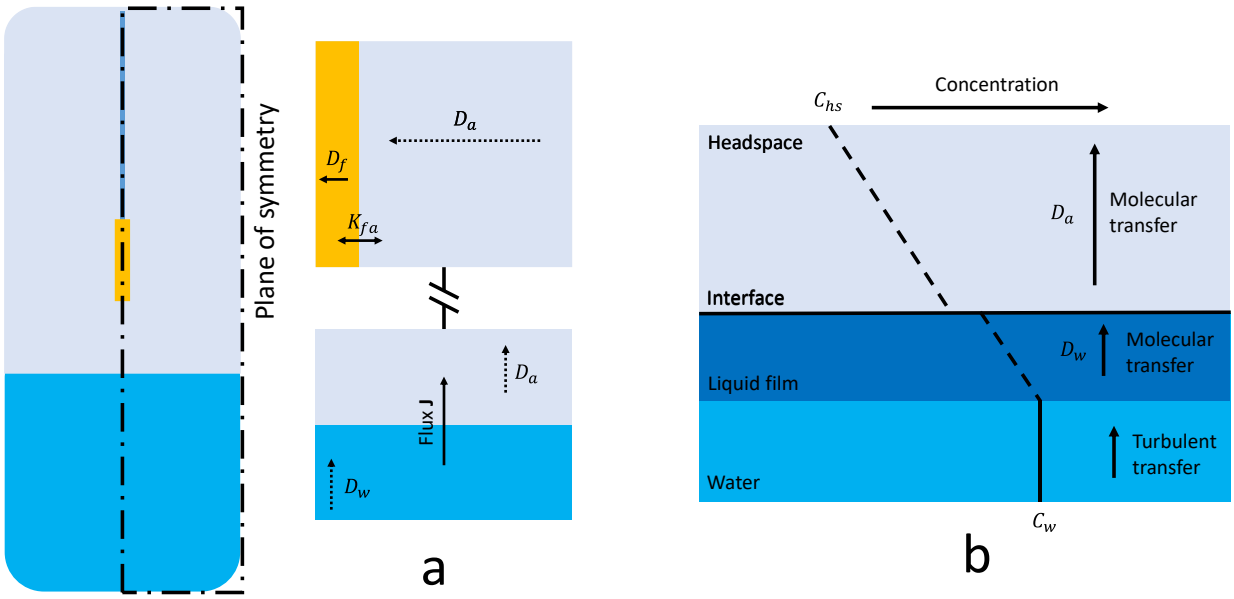


Figure 11 – Schematic representation of HSSPME of VOCs from water without agitation (a) and an analyte mass transfer process at the water-headspace boundary; (b) when agitation is used.

3.2.1 Adsorption from headspace to a porous coating

Adsorption of VOCs from headspace by a porous SPME fiber coating is a reversible process, which in the case of low analyte concentrations can be described by a coating-headspace distribution constant (K_{fh}) [112]:

$$K_{fh} = \frac{[C_f]}{[C_h]} \tag{33}$$

where $[C_f]$ and $[C_h]$ are equilibrium concentrations of an analyte in a coating and headspace, respectively. Value of the constant indicate the affinity of an analyte to a coating and depend on temperature. It can be determined experimentally or predicted.

Distribution constant between headspace and fiber Car/PDMS can be estimated using LSER approach by Prikryl et.al [127]

$$\log K_{fa} = 3.92(0.13) + 0.35(0.09)S - 0.36(0.14)A + 0.43(0.05)L \tag{34}$$

3.2.2 Mass transport in a porous coating

Kenessov et al. [124] modeled mass transport in a Car/PDMS coating using 'Transport of Diluted Species in Porous Medium' physics in CMP and the equation:

$$\left(\varepsilon + \rho\, K_p\right) \frac{\partial c}{\partial t} = D_e\, \nabla^2 \mathrm{c} \tag{35}$$

where: ε is a porosity of a porous material; ρ is a density of a porous material, kg m^{-3}; K_p is a distribution constant between coating and air, m^3 kg^{-1}; D_e is the effective diffusivity in the coating. Kenessov et al. [124] proved that for greater accuracy of the modeling, PDMS in Car/PDMS coating should be considered as a solid phase. For the modeling, the coating porosity and density were set to 0.366 and 760 kg m^{-3}, respectively. K_p (m^3 kg^{-1}) was calculated by dividing K_{fh} (dimensionless) by the coating density

3.2.3 Mass transport in aqueous phase and partitioning between headspace and aqueous phase

HSSPME of VOCs from aqueous samples can be conducted without and with agitation. Compared to air, liquid-phase diffusion coefficient is obligate to define solvent and solute liquid-phase mixture, where solute is considered as infinite dilution in the solvent. The theoretical background engaged to use Wilke and Chang [100] correlation in determination of diffusion in water for nonelectrolytes in infinitely dilute solution:

$$D_w(\mathrm{m^2\ s^{-1}}) = 7.4 \cdot 10^{-8} \frac{(\varphi\, M(\mathrm{H_2O}))^{1/2} T}{\mu V_a^{0.6}} \tag{36}$$

where φ is the association parameter of the solvent (2.26 for water), M (H_2O) is the molecular weight of water, μ is the dynamic viscosity of water (cP), V_a is the molar volume of an analyte at its normal boiling point (m^3 mol^{-1}).

A simpler Hayduk and Laudie [128] correlation can also be used:

$$D_w = 13.26 \times 10^{-5} {\mu_B}^{-1.14} {V_a}^{-0.589} \quad (37)$$

where D_w is the diffusion coefficient of analyte in solvent (water), $cm^2\ s^{-1}$; μ is the viscosity of water, cP; V_a is the molar volume of analyte at normal boiling point, $cm^3\ mol^{-1}$ that can be found by Tyn and Calus [129] equation, if experimental values are not available:

$$V_a = 0.285\ {V_c}^{1.048} \quad (38)$$

where V_c is the critical volume of analyte, cm^3/mol.

Flux of compounds from water to headspace (J) is calculated using [130]:

$$J = K_L \left(C_w - \frac{C_g}{K_{hw}} \right) \quad (39)$$

where C_h and C_w are the boundary concentrations of an analyte in the headspace and water, respectively, K_{hw} is the dimensionless Henry's law constant (HLC) – analyte distribution constant between headspace and water, which is defined as the ratio of equilibrium concentrations in the headspace and water, K_L is the flux coefficient that can be determined using [131]:

$$\frac{1}{K_L} = \frac{1}{k_w} + \frac{1}{k_h K_{hw}} \quad (40)$$

where k_h and k_w are the exchange constants for the headspace and water, respectively, which depend on the mass transport rate in respective phases.

Liss and Slater [131] established the values of exchange constants for sea surface:

$$k_h(\mathrm{H_2O}) = 3000\ \mathrm{cm\ h^{-1}},\ k_w(\mathrm{CO_2}) = 20\ \mathrm{cm\ h^{-1}} \quad (41)$$

Liss and Slater [131] also established that exchange constants are inversely proportional to the square root of the molecular weight of the solute:

$$k \sim M^{-1/2} \quad (42)$$

Therefore, above mentioned values should be further corrected to account for the molecular weight of the compound.

Southworth [132] have determined that for no wind conditions, and 200 RPM stirring with a propeller, the exchange constants for M = 100 are:

$$k_h = 539\ \mathrm{cm\ h^{-1}},\ k_w = 15.9\ \mathrm{cm\ h^{-1}} \quad (43)$$

For no wind conditions, Southworth [132] established the following equations to describe exchange constants:

$$k_h(\text{cm h}^{-1}) = 1137.5\, V_{\text{current}} \left(\frac{18}{M_r}\right)^{1/2} \quad (44)$$

$$k_w(\text{cm h}^{-1}) = 23.51\, \frac{V_{\text{current}}^{0.969}}{R^{0.673}} \left(\frac{32}{M_r}\right)^{1/2} \quad (45)$$

where $V_{current}$ is the current velocity (m s^{-1}), R is the stream depth (m).

Another possibility for modeling the mass transport of VOCs in aqueous phase under stirring is to use Computational Fluid Dynamics (CFD) module in CMP. Currently, there are no CFD module-based models for simulating HSSPME of VOCs from water. However, recently, Jafari et al. [133] developed the model for simulating DISPME of pyrene and phthalate esters from water under different stirring rates, which has the potential to be adopted for HSSPME modeling. 'Turbulent Flow, k-ε' physics was used along with a Reynolds-averaged Navier-Stokes (RANS) approach. In the geometry, the total swept volume of the rotating magnet (cylinder) was used instead of the volume of the magnet. External and upper walls of the cylinder were modeled rotating around the axis of the vial symmetry (in 2D-axisymmetric geometry). SPME was modeled using 'Transport of Diluted Species' physics (time-dependent study) with convection velocities taken from the results obtained using 'Turbulent Flow, k-ε' physics (stationary study).

3.2.4 Estimation of K_{hw} (HLC) values

In aqueous solutions, organic pollutants are present at low concentrations and governed by Henry's simple law, according to which in ideally dilute solutions, the vapor pressure of a solute is directly proportional to the concentration of a substance in a solution [134]. In this case, the coefficient of proportionality (Henry's law constant) is a function of several parameters, such as temperature, ionic strength of the solution, but is independent on the concentration of the solute itself [135]:

$$k_H^{px} = \lim_{x_i \to 0} \frac{f_i}{x_i} \quad (46)$$

where k_H^{px} is HLC, f_i and x_i are the fugacity and the mole fraction of the solute, respectively.

Fugacity of the gas can be estimated using [136]:

$$f_i = \gamma_i x_i p_i \quad (47)$$

where γ_i is the activity coefficient of the solute, p_i is the partial pressure of the solute. Therefore, HLC can be redefined as:

$$k_H^{px} = \lim_{x_i \to 0} \gamma_i p_i = \gamma_i^{\infty} p_i^{sat} \quad (48)$$

where γ_i^{∞} is the activity coefficient of the solute at infinite dilution, p_i^{sat} is the vapor pressure of the pure solute.

The dimensionless Henry constant is defined as the ratio of the molar concentrations of a solute in the gas and liquid phases at equilibrium:

$$K_{hw} = \frac{[C_h]}{[C_w]} \tag{49}$$

Therefore, for dilute mixture and ideal gas conditions, the following equation is true:

$$K_{hw} = k_H^{px} \frac{V_m}{RT} \tag{50}$$

where V_m is the molar volume of water (m^3 mol^{-1}) at temperature T (K), R is the gas constant (J mol^{-1} K^{-1}). Thus, dimensionless HLC can be calculated as:

$$K_{hw} = \gamma_i^{\infty} p_i^{sat} \frac{V_m}{RT} \tag{51}$$

Consequently, predicting the HLC of the solute is converged to calculating the activity coefficient of the compound at infinite dilution, since vapor pressure of pure substances can be estimated using extensive experimental data.

Activity coefficients of solutes can be calculated using the UNIFAC model [137], which is based on 3 main assumptions:

1) the logarithm of the activity coefficient is a sum of combinatorial (accounts for size and shape of the molecules) and residual (accounts for energy interactions) contributions:

$$\ln \gamma_i = \ln \gamma_i^C + \ln \gamma_i^R \tag{52}$$

2) the residual contribution is the sum of the individual contributions of each solute group:

$$\ln \gamma_i^R = \sum n_k^i (\ln \Gamma_k - \ln \Gamma_k^i) \tag{53}$$

k is a group in the molecule i, n_k^i is the number of groups k in the molecule i, Γ_k is the contribution of the group k in a mixture, Γ_k^i is the contribution of the group k in pure i.

3) each group contribution depends only on group concentration and temperature:

$$\Gamma_k = f(x_1, x_2 \ldots x_N, T) \tag{54}$$

The full equations of UNIFAC are not presented here, details may be found in [137].

3.3 Method

3.3.1 General modeling parameters

The geometry (Fig. 12) consisted of four main rectangular domains: water, headspace, fiber core (0.13 x 10 mm) and fiber coating (0.08 x 10 mm). A small additional rectangle (0.31 x 10.2 mm) was built around the coating as proposed by Kenessov et al. [124] for

improved modeling accuracy. Mass transport in water and headspace was modeled using Eq. (15). Mass transport and adsorption in the coating were modeled using Eq. (35). Fluxes of compounds from water to headspace were calculated using eq. (39). Backward fluxes (from headspace to water) were calculated using the same eq. (39) with the minus sign in front of the equation [124].

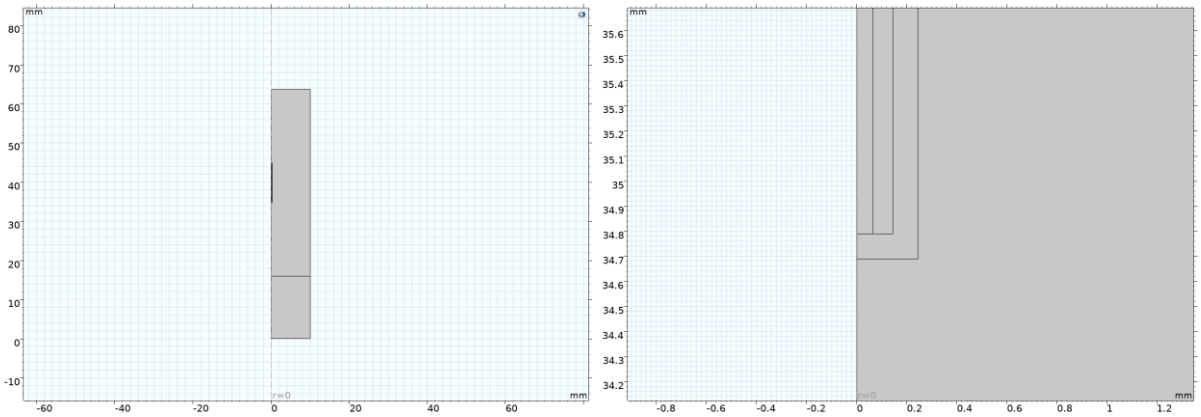


Fig. 12. Geometry of the model for 20 mL vial. Note: 1 – water, 2 – headspace, 3 – fiber core, 4 – fiber coating, 5 – headspace area where initial concentration was set to zero.

All modeling was conducted for 85 μm Car/PDMS coating (Supelco, USA), the structure of which was thoroughly studied before [124]. Coating porosity, tortuosity factor and bulk density were set to 0.366, 1.317 and 760 kg m^{-3}, respectively. User defined adsorption isotherm was chosen for the adsorption modeling using:

$$C_p = C\,K_p \tag{55}$$

where C_p is the concentration adsorbed to the solid material of the coating, mol kg^{-1}; C is the concentration in voids and pores of the coating, mol m^{-3}; K_p is the coating-headspace distribution constant, m^3 kg^{-1}.

Initial concentration of an analyte in water before extraction (C_{ow}) was calculated using:

$$C_{ow} = \frac{C_0\,V_w}{(K_{hw}\,V_h + V_w)} \tag{56}$$

where C_0 is the initial analyte concentration in water before introducing it to the vial; K_{hw} is the dimensionless headspace-water distribution constant; V_w and V_h are the volumes of water and headspace, respectively. C_{ow} is lower than C_0 because a part of the analyte will be transported to the headspace during pre-incubation. Initial concentrations of analytes in headspace before extraction (C_{oh}) was calculated by multiplying C_{ow} by K_{hw}. Initial analyte concentrations in the coating and small (0.31 x 10.2 mm) additional rectangle around the coating were set to zero.

The model included functions for calculating flux coefficient (K_L) values using three approaches described in section 2.4 (Liss and Slater [131] and Southworth [132]), D_h values using Fuller [102] method (eq. (14)), K_{fh} values using LSER approach (eq. (34)) [114], and

K_{hw} values using eq. (51). Input values for using these functions were provided as global parameters or calculated in CMP. Extraction temperature (298 K) and pressure (1 atm) were assumed constant and homogeneous in all domains. Fuller diffusion volume values were obtained from the 'Thermodynamics' database in CMP. Liquid system containing target solute and water in 'Thermodynamics' was defined in CMP. UNIFAC VLE was chosen as a thermodynamic model in CMP. Infinite dilution diffusion coefficients calculated with Wilke-Chang correlation were obtained from mixture properties. Infinite dilution activity coefficients were obtained from mixture properties, molar volume of water was obtained from species properties. In a separate gaseous system containing only target solute, natural logarithm of vapor pressure was calculated. HLC was calculated using the eq. (51). The processes were simulated for all studied analytes simultaneously. The list and values of parameters used for modeling are provided in Table .10-14.

Table 10. General modeling parameters

Parameter name	Value or formula for calculation	Description
CoreD	0.13[mm]	Core diameter
CoatTh	0.08[mm]	Coating thickness
VialD	20[mm]	Vial diameter
VialV	20[cm^3]	Vial volume
VialH	VialV*4/pi/VialD^2	Vial height
FiberDepth	HSH/2+5[mm]	Fiber insertion depth
WaterV	5[cm^3]	Water volume
WaterH	WaterV*4/pi/VialD^2	Water height
HSH	VialH-WaterH	Headspace height
CoatL	10[mm]	Coating length
T	298.15[K]	Temperature
p	1[atm]	Pressure
VelRPM	1000[1/min]	Stirring speed
VelTan	2*pi*VelRPM	Tangential velocity of magnetic stirrer
MrAir	28.97[g/mol]	Molar mass of air
DVair	20.1	Fuller diffusion volume of air
MrW	18.015[g/mol]	Molar mass of water
DVw	12.7	Fuller diffusion volume of water

Table 11. Coating parameters

Parameter name	Value or formula for calculation	Description
PartPor	0.37	Porosity of

		particles
PartDen	1000[kg/m^3]	Density of particles
InterPartPor	0.24	Inter-particle porosity
CoatPor	InterPartPor+PartPor*(1-InterPartPor-PDMS)	Coating porosity
PDMS	0.42	PDMS fraction
CoatDen	PartDen*(1-InterPartPor)	Coating density
CoatTort	CoatPor+1.5*(1-CoatPor)	Coating tortuosity factor

Table 12. Parameters of analytes for calculating coating-headspace distribution constants using LSER

Analyte	S	A	L
Benzene	0.52	0	2.786
Toluene	0.52	0	3.325
Ethylbenzene	0.51	0	3.778
o-Xylene	0.56	0	3.939

Table 13. Fuller diffusion volumes of analytes in headspace (calculated in CMP using 'Thermodynamics') and their diffusion coefficients in headspace at 1 atm and 0.0313 atm (calculated in CMP using function based on Fuller method)

Analyte	Fuller diffusion volume	D_h at 1 atm, $m^2 s^{-1}$	D_h at 0.0313 atm
Benzene	90.68	8.94e-6	3.83e-4
Toluene	111.48	7.35e-6	3.16e-4
Ethylbenzene	131.6	7.01e-6	3.03e-4
o-Xylene	131.6	7.01e-6	3.03e-4

Table 14. Infinite dilution activity coefficients of analytes in water, vapor pressures (calculated in CMP using 'Thermodynamics' and UNIFAC VLE), HLC values (calculated in CMP using function based on eq. (21)) and diffusion coefficients of analytes in water (calculated in CMP using 'Thermodynamics' and Wilke-Chang method)

Analyte	Infinite dilution activity coefficient in water	Vapor pressure, Pa	HLC	D_w ($m^2 s^{-1}$)
Benzene	2413	12713	0.224	8.59e-10
Toluene	12072	3812	0.335	9.59e-10
Ethylbenzene	33940	1289	0.319	8.17e-10
o-Xylene	33940	1126	0.279	8.84e-10

Extra fine free triangular mesh was used for the modeling. For better accuracy, resolution of narrow regions was increased to 10. For time dependent calculations, output times started from "range(0,0.1,1)" and continued till the equilibration at the step of 1 s. All other study settings were set to default (Physics controlled).

During data processing, surface average derived values were calculated. 'Concentration species absorbed to the solid' were used for calculating concentration in the coating. For headspace and water, surface average concentrations were calculated.

General accuracy of the modeling was checked by comparing computed equilibrium amounts of analytes (*n*) in the coating with those calculated using eq. (8) [112]:

3.3.2 Comparison of simulated and experimental profiles

Experimental profiles obtained by Popp and Paschke [138] were taken for comparison. They conducted HSSPME of benzene, toluene, ethylbenzene, *m*- and *o*-xylene (BTEX) from 5 mL of water sample (C_0 = 0.35 mg L^{-1}) in an 8.0 mL vial using 80 µm Car/PDMS fiber at 25 °C under magnetic stirring at 1000 RPM. Modeling was conducted as same parameters. Vial diameter was set to 14 mm. Upper end of the coating was located 5 mm from the vial top. Modeling was conducted only for benzene, toluene, ethylbenzene and *o*-

xylene.

Modeling was conducted using two different approaches for calculating exchange constants - Liss and Slater [131] and Southworth [132]. For the approach of Southworth [132], current velocity ($V_{current}$, m s^{-1}) was calculated automatically for each point of the water surface using:

$$V_{current} = 2\,\pi\,r\,S \tag{57}$$

where r is the distance from the vial axis of symmetry, m; S is the stirring rate, s^{-1}. Stream depth (R) was set to the height of water in the vial (~32.5 mm).

For testing approaches of Liss and Slater [131] and Southworth [132], D_w were set to 10^{-2} m s^{-2}. In this case, the diffusion in water did not affect the extraction process. To estimate the importance of the accurate modeling of the mass transfer at headspace-water boundary, the modeling was also conducted at very high K_L values (100 m s^{-1}).

The modeling was additionally conducted without stirring. In this case, D_w values were calculated using Wilke and Chang [100] method in CMP. Because in this case the process will be limited mainly by the mass transfer in water, K_L values were set to100 m s^{-1}.

3.3.3 Application of the developed model for optimization of extraction parameters

Modeling was conducted for a 20 mL vial with an internal diameter of 20 mm. The effect of stirring rate was studied at pressures 1 and 0.0313 atm; the coating was located in the center of the headspace. The effect of fiber insertion depth was studied at 1000 RPM stirring and 1 atm pressure. The effect of pressure was studied at 1000 RPM stirring and the coating located in the center of the headspace. The effect of water volume was studied at 1000 RPM stirring, 1 atm pressure and the coating located in the center of the headspace. The effect of concentration of added salt was studied at 1000 RPM stirring, 1 atm pressure, 5 mL water volume and the coating located in the center of the headspace. Headspace-water constants (K_{hw}) for benzene at different concentrations of added salt were determined experimentally by analyzing headspace over aqueous solutions of benzene without and with added salt (3 and 6 molL^{-1}) using gas chromatography-mass spectrometry (GC-MS). For the experiment, three 5-mL samples of distilled water in 20 mL vial were spiked with 1.00 µL of benzene solutions in methanol to obtain benzene concentrations of 180 ng mL^{-1}. To second and third sample, sodium chloride was added to obtain its concentrations 3 M and 6 M, respectively. After 1.5 h of preincubation at 30 °C, 100 µL of headspace sample was introduced into split/splitless inlet of the Agilent 7890A/5975C (Agilent, USA) GC-MS parameters were presented in section 2.3.2

HLC in a salt solution ($K_{hw,s}$) was calculated using:

$$K_{hw,s} = K_{hw}\frac{\frac{RV_w}{K_{hw}V_h+V_w-RK_{hw}V_h}}{} \tag{58}$$

where R is the ratio of responses of the analyte for benzene solution in water with and without salt addition, K_{hw} is the HLC for distilled water estimated using eq. (49), V_h and V_w

are the volumes of headspace and water, respectively.

Determined K_{hw} values for 3 and 6 mol/L of added NaCl were 0.40 and 0.62, respectively.

3.3.4 Optimization of incubation time

The developed model for HSSPME was corrected by removing other geometry parts except water and headspace. 'Transport of Diluted Species' was used for headspace instead of the 'Transport of Diluted Species in Porous Media'; the corrected model contained two 'Transport of Diluted Species' physics. Initial analyte concentration in headspace was set to zero.

3.4 Results and discussion

3.4.1 Comparison of simulated and experimental profiles

BTEX extraction profiles from water obtained using very large flux coefficients (K_L= 100 m s^{-1}) are substantially different from experimental profiles indicating that the mass transport of analytes from water to headspace affects the extraction process (despite high stirring speed) and cannot be ignored during the modeling (e.g., for its simplification). Simulated profiles obtained without stirring were substantially different from experimental profiles because extraction was limited by the slow diffusion in water. This indicates that stirring plays an important role in the extraction process of BTEX from water by Car/PDMS fiber.

Model BTEX extraction profiles from water obtained using two different approaches for calculating exchange constants are substantially different (Fig. 13). The method of Southworth [132] allowed obtaining extraction profiles, which are closest to the experimental profiles obtained by Popp and Paschke [138]. Greater accuracy of the approach of Southworth [132] over Liss and Slater [131] can be caused by the consideration of the greater number of factors.

When using Southworth [132] approach, root mean square deviation (RMSD) between experimental and simulated values for benzene, toluene, ethylbenzene and *o*-xylene were 5.5, 6.3, 10.4 and 6.0%, respectively. Previously [139], RMSD values below 10 were considered satisfactory. Thus, the proposed methodology with the Southworth [132] approach for estimating exchange constants can be recommended for modeling HSSPME of VOCs from water.

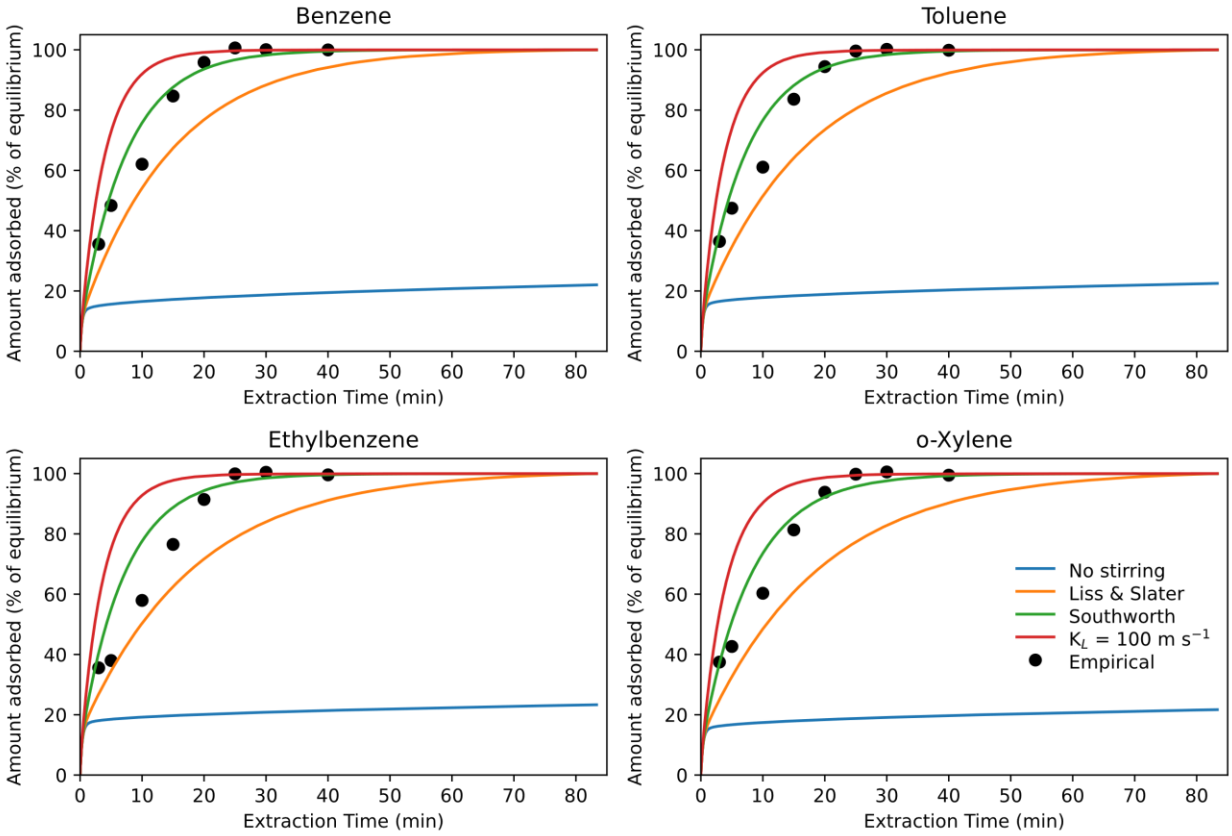


Figure 13 – Comparison of experimental [138] and simulated HSSPME profiles of BTEX from water (5 mL in 8 mL vial) by 85 μm Car/PDMS fiber

3.4.2 Application of the developed model for optimization of extraction parameters

The developed model can be used for studying the effect of extraction parameters (stirring speed, fiber location, pressure in the vial) on the extraction rate and finding parameters providing lowest possible equilibrium extraction time (Fig. 14). For example, increase of stirring speed from 500 to 1000 and 2000 RPM can provide a decrease in time required for extracting 95% of the equilibrium benzene amount ($t_{95\%}$) by 2.2 min (11%) and 3.2 min (16%), respectively (Fig. 14a). Fiber insertion depth (distance from the vial top to the coating tip) also provides a substantial effect on $t_{95\%}$: its increase from 15 to 20, 30 and 40 mm results in the decrease of $t_{95\%}$ by 2.0 (9.0%), 5.5 (25%) and 8.5 min (38%), respectively (Fig. 14b). Decreasing the pressure in the vial from 1 to 0.0313 atm (vapor pressure of water) results in the increase of $t_{95\%}$ by 14.3 min (83%) (Fig. 14c).

Because vacuum allows a strong increase in extraction rate, effects of stirring speed and fiber insertion depth were studied using the developed model under vacuum conditions. Increasing stirring speed from 500 to 1000 and 2000 RPM under vacuum conditions provides even greater effect on $t_{95\%}$ compared to extraction at 1 atm: it decreases by 2.5 (48%) and 3.8 min (71%), respectively (Fig. 14d). Fiber insertion depth has no effect on the benzene extraction profiles under vacuum conditions (data are not shown). Thus, the developed method allows optimization Vac-HSSPME.

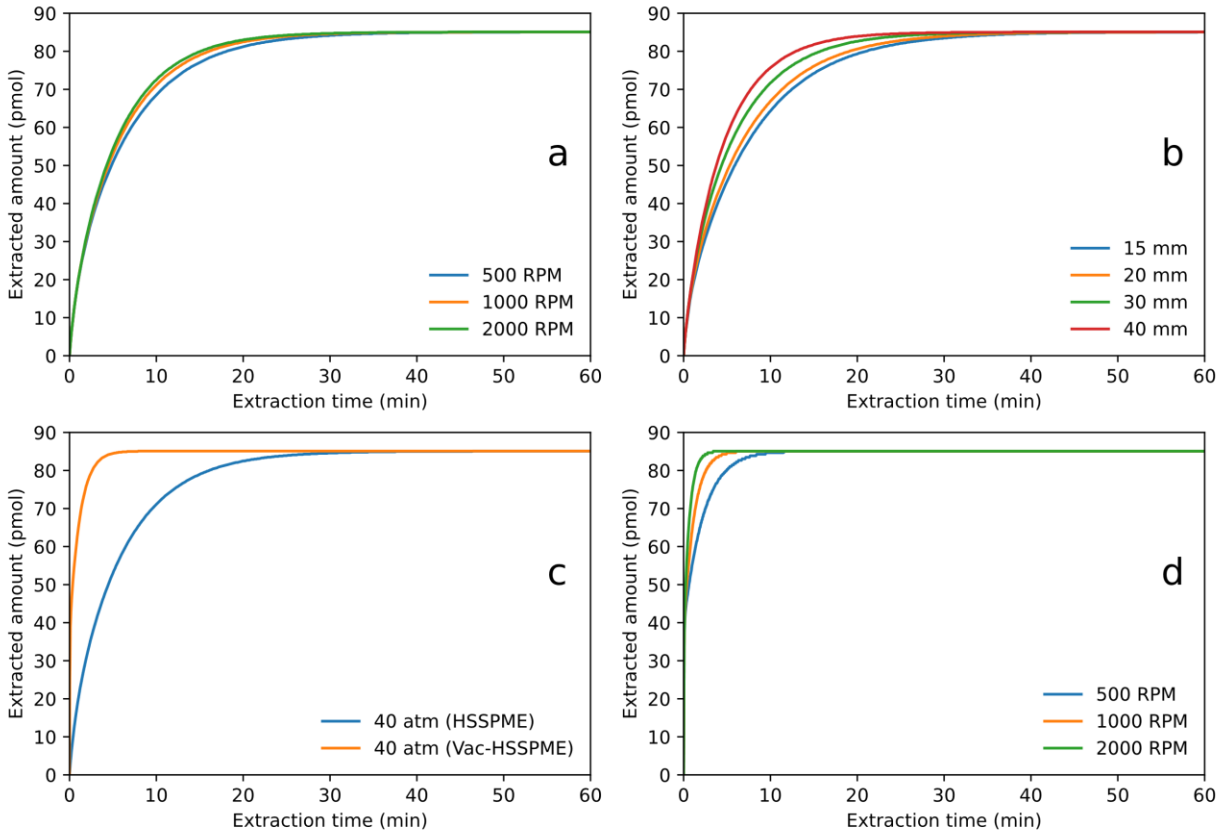


Figure 14 – Effect of stirring rate (a), fiber insertion depth (b), vacuum (c) and stirring rate under vacuum (d) on benzene extraction profiles from water (5 mL in 20 mL vial) by 85 µm Car/PDMS fiber

Often the extraction time should be set at the "linear" range of the extraction profile, long before the equilibrium is established, e.g., to minimize the competition between analytes and matrix compounds for better accuracy [112]. In addition, it can take a very long time till the equilibrium is established (particularly, for analytes with low K_{hw} and high K_{fh} [140]) and using non-equilibrium extraction is more practically feasible.

Using the developed model, water volume can be optimized for a greater extracted amount at any extraction time (Fig. 15a). At all studied extraction times (5, 10 and 30 min), increase in water volume results in the increase of extracted amount. However, this effect is more pronounced at higher extraction times. Effect of the concentration of added salt can also be studied using the modeling, but it requires knowing K_{hw} values at each salt concentration. For benzene, determined K_{hw} values at concentrations of NaCl 3 and 6 $molL^{-1}$ were 0.40 and 0.62 (1.8 and 2.8 times higher than without addition of salt, respectively). According to the results of modeling, at extraction time 5 min, addition of 3 and 6 mol/L NaCl resulted in the 26 and 40% increase of the extracted amount of benzene (Fig. 15b). At extraction time 30 min, the effect of salting out was much less pronounced and resulted in the increase only by 8 and 11% for 3 and 6 mol/L NaCl, respectively.

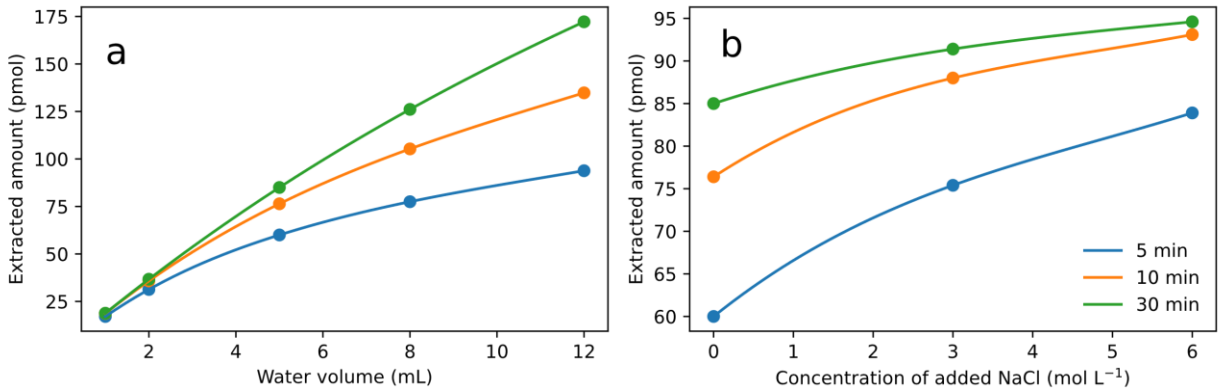


Figure 15 – Effect of water volume (a) and concentration of added NaCl (b) on extracted amounts of benzene from water by 85 µm Car/PDMS fiber after different times of HSSPME

3.4.3 Optimization of preincubation time

After minor modification of the developed model (removal of the coating), it is possible to use for optimization of preincubation time, which is another important parameter optimized experimentally. Preincubation is necessary for establishing the equilibrium between headspace and aqueous phase after introducing a water sample to the vial. During this process, mass transfer of an analyte from aqueous phase to headspace occurs resulting in the increase of an analyte concentration in headspace and decrease of its concentration in aqueous phase.

Results of the modeling showed that preincubation rate of water samples before HSSPME of benzene depends on the stirring speed (Fig.16): at 500 RPM, 95% of equilibrium benzene concentration in headspace is achieved in 5.8 min, at 1000 RPM – in 4.4 min, at 2000 RPM – in 3.7 min.

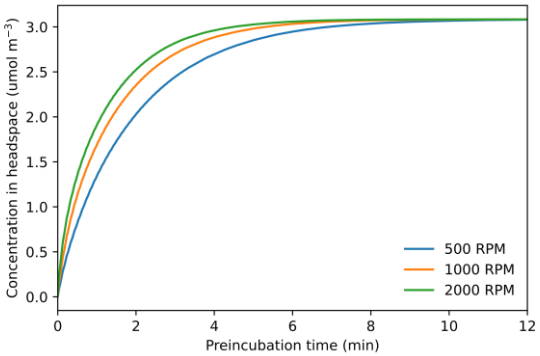


Figure 16 – Effect of stirring speed on preincubation of 5-mL water samples in 20 mL vial before HSSPME of benzene

3.5 Conclusion on the section

Thus, the new model for simulating headspace solid-phase microextraction of volatile organic compounds from water samples with porous coatings was developed using finite element analysis platform COMSOL Multiphysics®. The model is mainly based on existing theory and previous research on the numerical modeling of SPME. Southworth approach

allowed obtaining BTEX extraction profiles from water, which were closest to experimental profiles compared to other approaches. Compared to other approaches, this approach takes into account the impact of stirring speed and depth of the water sample. In addition, it was developed at the conditions, which are very similar to those of HSSPME from water.

The developed model was successfully applied for computational optimization of extraction and parameters for HSSPME of BTEX – stirring speed, fiber insertion depth, pressure, sample volume and the concentration of added salt. It has been shown that Vac-HSSPME of benzene from water is substantially faster than HSSPME under atmospheric pressure. The effect of stirring rate was much more pronounced during Vac-HSSPME, while fiber insertion depth showed no effect on benzene extraction profile from water under vacuum. Preincubation time of water sample before HSSPME was also successfully optimized after minor changes in the model.

The developed model can be recommended for optimization of HSSPME- and Vac-HSSPME-based analytical methods for VOCs quantification in water. Optimization of stirring speed, fiber location, pressure, sample volume and vial geometry is possible without additional experiments. For optimization of salt concentration and pH, K_{hw} values at corresponding conditions should be determined experimentally. In the future research, the model can be improved by including the effects of temperature and pH of water sample.

4 DEVELOPMENT AND APPLICATION OF COMPUTATIONAL MODELS FOR SIMULATING HEADSPACE SOLID-PHASE MICROEXTRACTION OF ORGANIC COMPOUNDS FROM SOIL

Preamble

The materials in this chapter have been published as research article: Bulat Kenessov, Anel Kapar; Optimization of solid-phase microextraction of volatile organic compounds from dry soil samples by porous coatings using COMSOL Multiphysics; *Chemical Bulletin of Kazakh national university*, 2022. № 4. P. 4–12. https://doi.org/10.15328/cb1300

4.1 Introduction

Fick's second law of diffusion has been used to model mass transport in the gas phase. Mass transport in a porous coating has been modeled Eq. (35). D_e is the effective diffusivity in the coating, $m^2\ s^{-1}$, that can be determined using:

$$D_e = D\ \varepsilon\ \ \sigma^{-1} \tag{59}$$

where: σ is the tortuosity factor of the coating (1.317 for 85 µm Car/PDMS [124]) that is calculated from the corresponding porosity [141].

To our best knowledge, the modeling of HSSPME of VOCs from soil samples has not been described in the open literature. This research was aimed at developing the model for simulation of HSSPME of VOCs from dry soils. Modeling mass transport and adsorption of VOCs in dry soils should be similar to that in porous coatings because both of them are saturated with gas. Wet soils contain or are saturated with water, which will require developing of a different, more complex model.

4.2. Methods

4.2.1 Modeling of HSSPME

Two-dimensional (2D) axisymmetric model was built using 'Transport of Diluted Species in Porous Media' physics. The geometry (Fig. 17) consisted of four main rectangular domains: soil, headspace, fiber core (0.13 x 10 mm) and fiber coating (0.08 x 10 mm). A small additional rectangle (0.31 x 10.2 mm) was built around the coating as proposed by Kenessov et al. [124] for improved modeling accuracy. Fiber core and coating were located in the center of the headspace. Mass transport in the headspace was modeled using Eq. (15). Headspace was considered static.

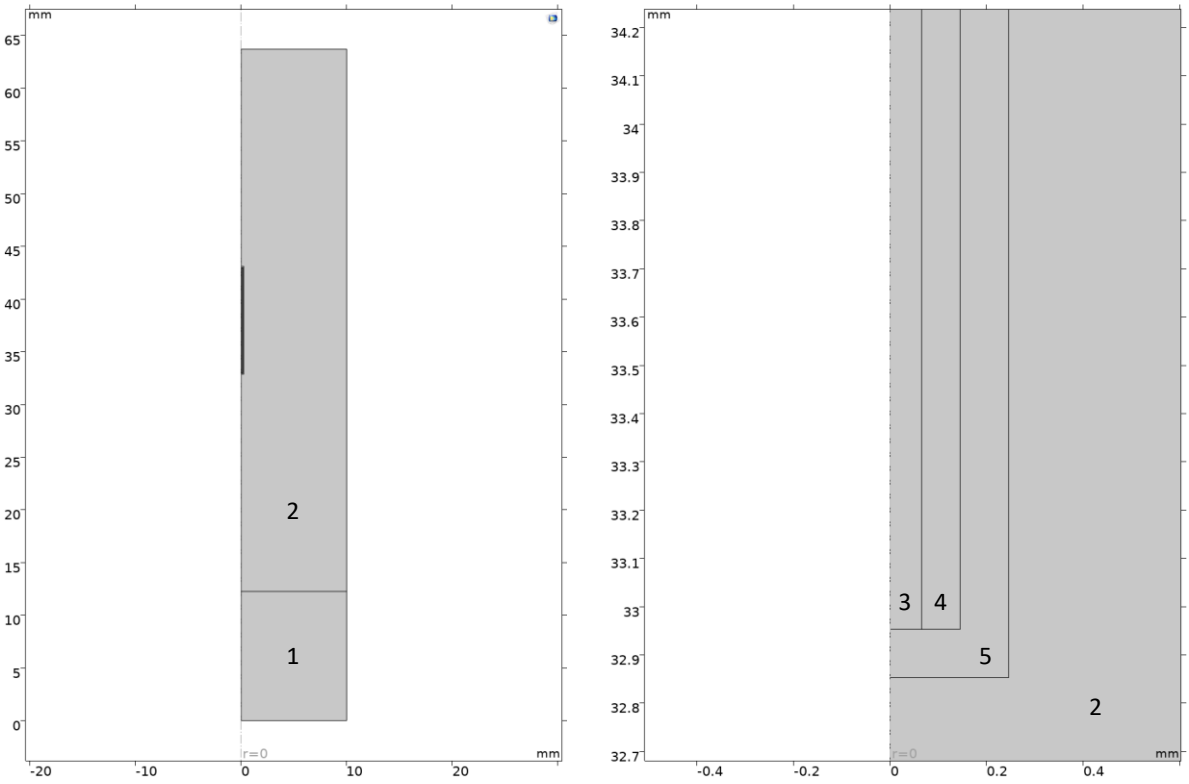


Figure 17 - Geometry of the model for solid-phase microextraction of VOCs from soil. Geometry components: 1 – soil, 2 – headspace, 3 – fiber core, 4 – SPME coating, 5 - additional rectangle around the coating where the initial concentration was set to zero.

Modeling was conducted for 85 µm Car/PDMS coating, the structure of which was thoroughly studied before [124]. Coating porosity, tortuosity factor and bulk density were set to 0.366, 1.317 and 760 kg m^{-3}, respectively. Porosity, tortuosity factor and bulk density of soil were set to 0.4, 1.3 and 1300 kg m^{-3}, respectively. User defined adsorption isotherm was chosen for the adsorption modeling using:

$$C_p = C\,K_p \tag{60}$$

where C_p is the concentration adsorbed to the solid material, mol kg^{-1}; C is the concentration in gas inside a solid material, mol m^{-3}; K_p is the solid-headspace distribution constant, m^3 kg^{-1}, calculated from the dimensionless solid-headspace constant (K_{sh}) using:

$$K_p = \frac{K_{sh}-\varepsilon}{\rho} \tag{61}$$

It was assumed that before HSSPME, the equilibrium between soil and headspace was established. Initial concentration of an analyte in headspace and soil gas before extraction (C_{oh}) was calculated using:

$$C_{oh} = \frac{C_{0s}\,m_s}{(K_{ps}\,m_s+V_h+\varepsilon_s m_s/d_s)} \tag{62}$$

where C_{0s} is the initial analyte concentration in soil before introducing it to the vial (mol/kg); K_{ps} is the soil-headspace distribution constant, $m^3\ kg^{-1}$; m_s and d_s are the mass (kg) and the bulk density ($kg\ m^{-3}$) of soil, respectively, V_h is the headspace volume (m^3), ε_s is the soil porosity. Initial analyte concentrations in the coating and small rectangle around the coating were set to zero.

Benzene was chosen as a model analyte for study. Two coating-headspace distribution constants (K_{fh}) were tested – 150000 and 8300, as reported by Prikryl and Sevcik [114] for 85 µm Car/PDMS and 65 µm PDMS/DVB fibers, respectively. Because the internal structure of PDMS/DVB is not reported in the available literature, parameters (dimensions, porosity, tortuosity factor and bulk density) for Car/PDMS were used for calculations at K_{fa} = 8300. Modeling was conducted using seven different dimensionless soil-headspace constants (K_{sh}): 1, 10, 100, 1000, 10,000, 100,000 and 1000,000.

Diffusion coefficient of benzene in headspace was calculated using Eq. (14). Extraction temperature (298 K) and pressure (1 atm or 0.0313 atm) were assumed constant and homogeneous in all domains. Fuller diffusion volume values were obtained from the 'Thermodynamics' database in CMP. Fluid diffusion coefficients of benzene in gas inside the coating and the soil were set equal to the diffusion coefficient in headspace.

Extra fine free triangular mesh was used for the modeling. For better accuracy, resolution of narrow regions was increased to 10 and maximum element size was set to 0.2. All other study settings were set to default (Physics controlled).

During data processing, surface average derived values were calculated. 'Concentration species absorbed to the solid' were used for calculating concentration in the coating. Relative concentrations in the coating were calculated by dividing computed concentrations absorbed to the coating by equilibrium concentrations calculated using [112]:

$$C_f = \frac{K_{fh} C_{0s} m_s}{K_{fh} V_f + K_{sh} m_s + V_h} \tag{63}$$

where V_f is the SPME coating volume ($5.28 \cdot 10^{-10}\ m^3$).

4.2.2 Modeling of pre-incubatio

Two-dimensional (2D) axisymmetric model was built using two 'Transport of Diluted Species' physics. The geometry consisted of two main rectangular domains: soil and headspace. Diffusion coefficient was set for simulating mass transport in soil [124]:

$$D_a = \frac{D\,\varepsilon}{\sigma\, K_{fh}} \tag{64}$$

Fluxes to (or backward from) headspace ($Flux_1$ and $Flux_2$, respectively) at the soil-air boundary were set to [124]:

$$Flux_1 = 1000\frac{m}{s}(c_s - c_h K_{sh});\ Flux_2 = 1000\ \frac{m}{s}(c_h K_{sh} - c_s) \qquad (65)$$

where: 1000 m s^{-1} is the flux coefficient at the soil-headspace interface (set to a very high value as previously used [124]); c_s and c_h are concentrations of the analyte in soil and headspace at the interface, respectively, mol m^{-3}. Initial analyte concentration in headspace was set to zero.

Relative concentrations in the coating were calculated by dividing computed concentrations absorbed to the coating by equilibrium concentrations calculated using [112]:

$$C_f = \frac{C_{0s}V_s}{(K_{sh}V_s + V_h)} \qquad (66)$$

4.3 Results and Discussion

4.3.1 Extraction profiles obtained during the modeling

The model allowed obtaining extraction profiles of benzene from headspace above soil (Fig. 18) using different values of the coating-headspace and soil-headspace distribution constants. At K_{fh} = 150,000, the increase of K_{sh} from 100 to 1000 resulted in a substantially longer equilibration process. Time required for extracting 95% of the equilibrium benzene amount ($t_{0.95}$) increased from 33.7 to 65.3 min. At K_{fh} = 8,300, the increase of K_{sh} from 100 to 1000 resulted in the increase of $t_{0.95}$ from 4.4 to 5.9 min. Equilibration at K_{fh} = 150,000 takes about one order of magnitude longer time than at K_{fh} = 8,300.

Such extraction profiles can be used for optimizing extraction time, which is typically chosen after the equilibrium is established. However, to minimize competition between analytes and matrix ingredients, extraction can be conducted at the linear range – when analyte concentration in a coating linearly increases with the increase of time [112].

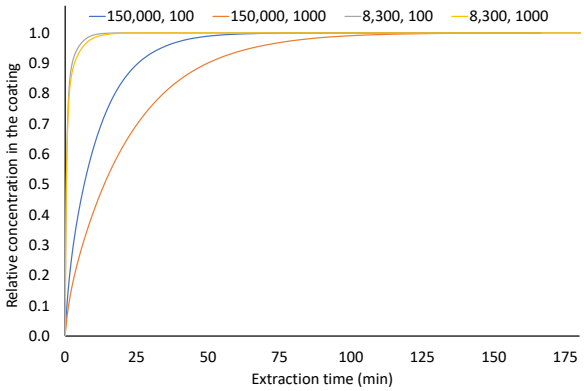


Figure 18 – Benzene solid-phase microextraction profiles from headspace above 1.00 g of soil in 20 mL vial at 1 atm simulated in CMP using two different K_{fh} (150,000 and 8,300) and K_{sh} (100 and 1000) values

4.3.2 Effect of sample mass under atmospheric pressure

Sample mass is an important parameter in HSSPME. Increase in a sample mass can result in an increased analyte amount in a coating and a lower detection limit. This

parameter is particularly important when extraction effectiveness is high [112]. However, the increase of soil mass and height in the vial can slow down the equilibration process, which will be more affected by the mass transfer in soil - analytes located at the bottom of the vial will have to pass via a thicker level of soil to reach the headspace. In the case of HSSPME of VOCs from water, mass transfer in the sample can be enhanced by stirring, but this approach is impossible for soil. According to Eq. (60), the mass transfer rate in soil depends on the fluid diffusion coefficient, porosity, tortuosity factor and soil-headspace distribution constant.

CMP allows simulating the effect of soil mass on extraction profiles and optimization of this important parameter along with extraction time (Figure 19). At K_{fh} = 150,000 and K_{sh} = 1, sample mass has a minor effect on the equilibration time (Figure 19A). At K_{fh} = 150,000 and K_{sh} = 10, linear dependence of $t_{0.95}$ on the sample mass is observed. At K_{fh} = 150,000 and K_{sh} = 100, linear dependence of $t_{0.95}$ on the sample mass is observed when increasing m_s from 2 to 10 g. At K_{fh} = 150,000, K_{sh} = 100 and m_s = 10 g, $t_{0.95}$ reaches 97.0 min, the highest value in this study. At K_{fh} = 150,000, K_{sh} = 100,000 and 1000,000, $t_{0.95}$ linearly decreases from 69.8-71.5 min to 52.3-54.0 min with the increase in m_s from 1 to 10 g. At K_{fh} = 150,000 and K_{sh} = 10,000, $t_{0.95}$ linearly decreases from 74.0 to 59.8 min with the increase in m_s from 2 to 10 g. At K_{fh} = 8,300, $t_{0.95}$ values are not higher than 6 min meaning that equilibrium extraction can be conducted at any m_s with low time expenses (Figure 19B). The trends are similar to those at K_{fh} = 150,000, except at K_{sh} = 100: $t_{0.95}$ increases when increasing m_s from 1 to 5 g followed by the decrease when m_s is increased to 10 g. At K_{fh} = 150,000 and K_{sh} = 1000, $t_{0.95}$ increases when increasing m_s from 1 to 5 g followed by a slight decrease when m_s is increased to 10 g.

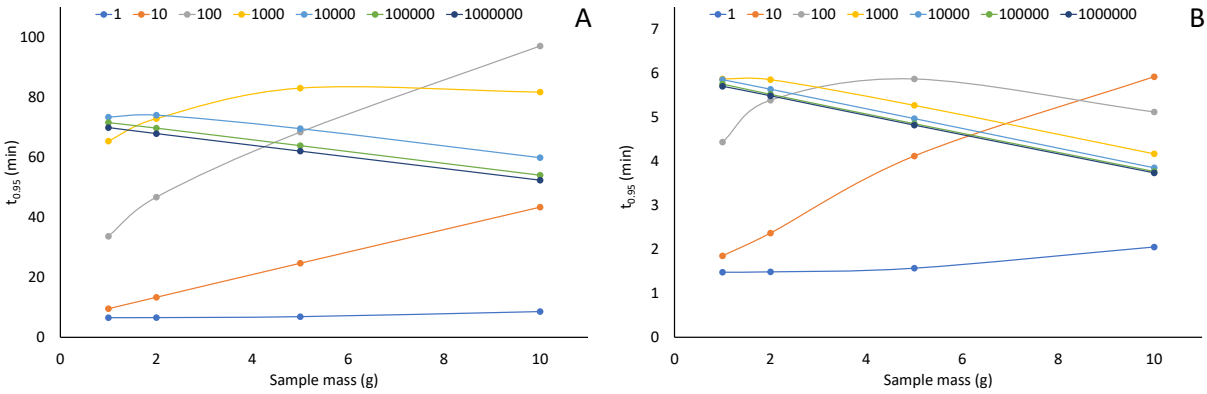


Figure 19 – Time required for extracting 95% of the equilibrium benzene amount ($t_{0.95}$) using coating-headspace distribution constants 150000 (A) and 8300 (B) at 298 K, 1 atm and different soil-headspace distribution constants

4.3.3 Effect of sample mass under vacuum conditions

HSSPME under vacuum conditions (Vac-HSSPME) can be used to achieve equilibrium faster [142–145]. This is mainly caused by the decreased diffusion coefficients in headspace under vacuum conditions [146]. The effect of vacuum when extracting VOCs from a dry soil is even more pronounced because it enhances mass transfer in the soil sample. As is seen from Equation (63), effective diffusion coefficient in soil is directly

proportional to the diffusion coefficient in soil gas that is the same as headspace. To estimate the effect of vacuum on $t_{0.95}$, a pressure in the model was set to 0.0313 atm corresponding to the saturated pressure of water at 298 K, benzene diffusion coefficient at 0.0313 atm was calculated and used in the modeling.

At K_{fh} = 150,000, $t_{0.95}$ under vacuum were 0.15-2.3 min at all studied K_{sh} and m_s values (Figure 20A). The trends were similar to those at atmospheric pressure, and $t_{0.95}$ under vacuum were 42-43 times lower than under atmospheric pressure. At K_{fh} = 8,300, $t_{0.95}$ under vacuum were 0.04-0.14 min at all studied K_{sh} and m_s values (Figure 20B). The trends were also similar to those at atmospheric pressure, and $t_{0.95}$ under vacuum were 42-43 times lower than under atmospheric pressure. The obtained results prove that the decrease of pressure in the vial substantially increases equilibration time at all studied values of distribution constants and sample masses. CMP can be used to estimate the effect of vacuum and optimize extraction time under vacuum conditions.

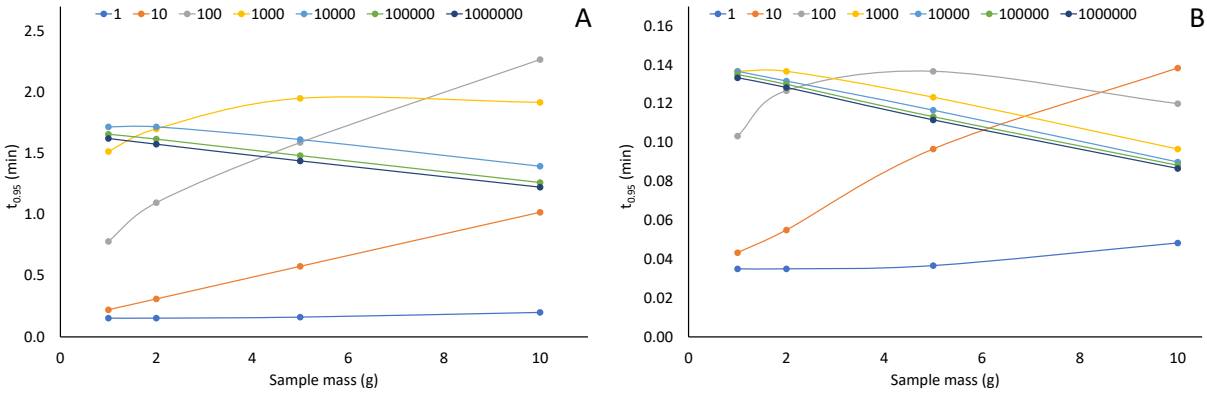


Figure 20 – Time required for extracting 95% of the equilibrium benzene amount ($t_{0.95}$) using coating-headspace distribution constants 150000 (A) and 8300 (B) at 298 K, 0.0313 atm and different soil-headspace distribution constants

4.3.4 Optimization of pre-incubation time

Pre-incubation time is an important parameter for achieving greatest accuracy and precision of methods based on HSSPME. It is required to establish the equilibrium between a sample and headspace in a vial before introducing and exposing an SPME fiber. Typically, pre-incubation time is optimized experimentally. Recently, CMP has been successfully used for optimization of preincubation time before HSSPME of VOCs from a water sample [147]. The model developed for HSSPME of VOCs from soil has been modified for optimization of pre-incubation time by removing SPME fiber and related domains from the geometry and physics. However, it was impossible to accurately set the initial concentration of the analyte in soil and soil gas, and another model was built using two 'Transport of Diluted Species' physics (for soil and headspace).

According to the modeling results, equilibration time ($t_{0.95}$) depends on both sample mass and soil-headspace distribution constant of the analyte (Fig. 21). At K_{sh} = 1 and 10, $t_{0.95}$ increases linearly with the increase of sample mass. At K_{sh} = 100, $t_{0.95}$ increases linearly only in the range from 1 to 5 g followed by a decrease. At K_{sh} = 1000, 10,000 and 1000,000, $t_{0.95}$ decreases linearly when increasing a sample mass from 2 to 10 g. At K_{sh} = 100,000, $t_{0.95}$

decreases linearly in the whole studied range of sample mass. Thus, the developed model can be used for optimizing the pre-incubation time.

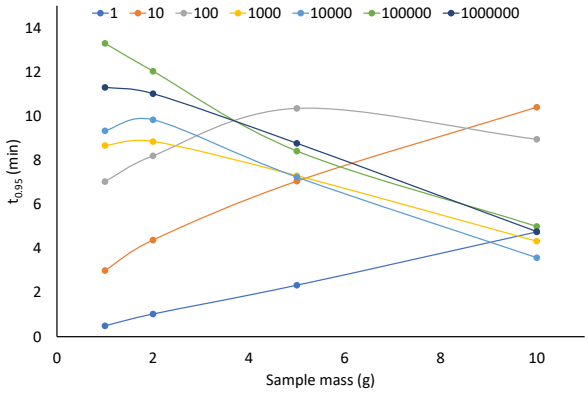


Figure 21 – Effect of sample mass on the time required for achieving 95% of the equilibrium of benzene between headspace and soil ($t_{0.95}$) at 298 K, 1 atm and different soil-headspace distribution constants

4.4 Chapter conclusion

Thus, a new CMP model has been developed for optimizing HSSPME of VOCs from dry soil samples. For optimization, coating-headspace and soil-headspace distribution coefficients at the extraction temperature, coating and soil porosities and bulk densities should be known. Fluid diffusion coefficients can be estimated using Fuller method. Extraction time and pressure can be optimized using the model. It was established that equilibrium in the system can be reached faster at 2.3 min under vacuum conditions (0.0313 atm), while equilibrium under atmospheric pressure (1 atm) is reached at 97 min for benzene. Sample mass from 2 g to 10 g does not affect on the distribution coefficients under 1000 except 10 and effect decreasing from 1000 to 1000000 at 2 g at coating-headspace distribution constants 150000 of benzene. At K_{fh} = 8300 the equilibrium extraction can be carried out in any sample mass with low time. It was established that pre-incubation time depends on the soil-headspace distribution constant that were studied during the modelling. Pre-incubation time can also be optimized after a minor modification of the main model because of the impossibility to set the initial concentration of the analyte in soil.

The developed model can be improved by considering soils saturated and unsaturated with water, which can be done using the ‘Unsaturated Porous Medium’ feature in the ‘Transport of Diluted Species in Porous Medium’ physics. Such modeling will require soil-water distribution constants, diffusion coefficients in water and volatilization rates for studied analytes. In addition, the model can be improved by adding a possibility of temperature optimization that will dependences of most modeling parameters on the temperature. The presented model is available to be used for optimization of solid-phase microextraction of all VOC compounds by providing the physico-chemical data.

CONCLUSION

In this research, computational models were developed using the finite element analysis platform COMSOL Multiphysics® based on existing theories and models to simulate solid-phase microextraction of volatile organic compounds from air, water, and soil under various parameters.

The developed computational model for SPME from air using a polydimethylsiloxane coating enables the simulation of VOC extraction profiles to optimize extraction times under different temperatures, pressures, sample volumes, and geometries, at constant or changing conditions;

The developed model of HSSPME- and Vac-HSSPME of BTEX from water by porous coating Car/PDMS can be used for optimization of stirring speed, fiber location, pressure, sample volume and vial geometry;

The developed computational model of SPME of VOCs by Car/PDMS coating from dry soil can be used for optimization of sample mass, location of the fiber, extraction time and pressures;

Fuller method was chosen for calculating diffusion coefficients of analytes in air due to its simplicity and reliability. Fiber-air distribution constants at different temperatures were estimated using van't Hoff equation. Southworth approach has been chosen for estimation of mass transfer coefficients at water-headspace boundary. The extraction profiles of BTEX from water obtained due to this approach were closest to obtained experimental profiles and reported in the literature. Compared to other approaches, this approach takes into account the impact of stirring speed and depth of the water sample.

In developing numerical models for SPME of VOCs from water samples, the LSER (Linear Solvation Energy Relationships) approach was utilized to estimate distribution coefficients between the fiber and headspace.

As a result, the following statements has been conducted:

The computational optimization of temperature and time of solid-phase microextraction of VOCs from air can be achieved using prediction techniques of Fuller method for diffusion coefficients in air, LTPRI indices and van't Hoff equation for estimation of distribution constants between headspace and fiber, and IGC for diffusion in PDMS with RMSDs in the range between 4.5% to 13.3% compared to obtained experimental extraction profiles of BTEX at 25°C and 40°C. Diffusion in the coating is a limiting stage in the extraction process at lower distribution constant between coating and air.When coating-air distribution constant equals to 10^3 the decrease of diffusion in the PDMS coating from $2 \cdot 10^{-9}$ m^2 s^{-1} to 10^{-11} m^2 s^{-1}, results the increase of the equilibration time from 6.5 to 32.6 seconds for extracting 80% of benzene at 25°C. At coating-air distribution constant equals to 10^5 similar decrease diffusion in the PDMS coating results increase from 46 to 66 seconds of equilibration time of benzene.

Vac-HSSPME provides faster equilibration compared to HSSPME for all (with any K_{fh} and HLC) VOCs from water at 298K under ideal stirring conditions by Car/PDMS coating. Increase of stirring speed from 500 to 1000 and 2000 RPM allows to decrease equilibration time ($t_{95\%}$) of benzene extraction from water by 2.5 (48%) and 3.8 min (71%), respectively under vacuum conditions. Southworth approach for estimating mass transfer coefficients at water-headspace boundary allows computational optimization of extraction time of SPME from water with RMSDs in the range 8.8-10% compared to experimental extraction profiles.

Equilibration time of benzene extraction by Car/PDMS coating from dry soil at Vac-HSSPME (0.0313 atm) can be reached faster at 2.3 min compared to traditional HSSSPME, where equilibrium under atmospheric pressure (1 atm) is reached at 97 min Equilibration time ($t_{0.95}$) depends on both sample mass and soil-headspace distribution constant of the analyte For the small sample masses less than 5 g, and soil-headspace distribution constants less than 100, equilibrium in the system can be achieved less than after 1 min of benzene extraction at K_{fh}=150 000 and less than 0.1 min at K_{fh}=8300 by Car/PDMS porous coating at 298K under vacuum conditions. For soil-headspace distribution constants more than 10^5 equilibration at the same time can be achieved for the sample mass of 10

REFERENCES

1 Pandey P., Yadav R. A Review on Volatile Organic Compounds (VOCs) as Environmental Pollutants: Fate and Distribution // INTERNATIONAL JOURNAL OF PLANT AND ENVIRONMENT. International Society of Environmental Botanists, 2018. Vol. 4, № 02. P. 14–26.

2 Pandey P., Yadav R. A Review on Volatile Organic Compounds (VOCs) as Environmental Pollutants: Fate and Distribution // INTERNATIONAL JOURNAL OF PLANT AND ENVIRONMENT. International Society of Environmental Botanists, 2018. Vol. 4, № 02. P. 14–26.

3 Regan S., Hynds P., Flynn R. Synthèse sur le carbone organique dissous dans l'eau souterraine et implications pour la sécurité de l'eau potable // Hydrogeol J. Springer Verlag, 2017. Vol. 25, № 4. P. 959–967.

4 Technologies A., Mavandadi F. Analysis of Benzene and its Derivatives (BTEX) in Water by Gas Chromatography.

5 Zalel A., Yuval, Broday D.M. Revealing source signatures in ambient BTEX concentrations // Environmental Pollution. 2008. Vol. 156, № 2. P. 553–562.

6 Guidance for Benzene in Residential Indoor Air Science Assessment Document.

7 Schupp T. et al. Benzene and its methyl-derivatives: Derivation of maximum exposure levels in automobiles // Toxicol Lett. Elsevier Ireland Ltd, 2006. Vol. 160, № 2. P. 93–104.

8 Begou P., Kassomenos P. One-year measurements of toxic benzene concentrations in the ambient air of Greece: An estimation of public health risk // Atmos Pollut Res. Elsevier B.V., 2020. Vol. 11, № 10. P. 1829–1838.

9 Khillare P.S. et al. Temporal variability of benzene concentration in the ambient air of Delhi: A comparative assessment of pre- and post-CNG periods // J Hazard Mater. 2008. Vol. 154, № 1–3. P. 1013–1018.

10 Ib Andersen by et al. Human response to controlled levels of toluene in six-hour exposures // Scand j work environ health. 1983. Vol. 9. 405–418 p.

11 Atsdr. Toxicological Profile for Toluene. 2017.

12 cannella2007.

13 Fishbein L. AN OVERVIEW OF ENVIRONMENTAL AND TOXICOLOGICAL ASPECTS OF AROMATIC HYDROCARBONS IV. ETHYLBENZENE // The Science of the Total Environment. 1985. Vol. 44. 269–287 p.

14 Tang W., Hemm I., Eisenbrand G. Estimation of human exposure to styrene and ethylbenzene // Toxicology. 2000. Vol. 144.

15 Wang P., Zhao W. Assessment of ambient volatile organic compounds (VOCs) near major roads in urban Nanjing, China // Atmos Res. 2008. Vol. 89, № 3. P. 289–297.

16 Li A.J., Pal V.K., Kannan K. A review of environmental occurrence, toxicity, biotransformation and biomonitoring of volatile organic compounds // Environmental Chemistry and Ecotoxicology. KeAi Communications Co., 2021. Vol. 3. P. 91–116.

17 Atsdr. TOXICOLOGICAL PROFILE FOR XYLENE. 2007.

18 Amini H. et al. Spatiotemporal description of BTEX volatile organic compounds in a Middle Eastern megacity: Tehran Study of Exposure Prediction for Environmental Health Research (Tehran SEPEHR) // Environmental Pollution. Elsevier Ltd, 2017. Vol. 226. P. 219–229.

19 Wang S. et al. Air pollutants in rural homes in Guizhou, China - Concentrations, speciation, and size distribution // Atmos Environ. 2010. Vol. 44, № 36. P. 4575–4581.

20 Hackbarth F. V. et al. Benzene, toluene and o-xylene (BTX) removal from aqueous solutions through adsorptive processes // Adsorption. Kluwer Academic Publishers, 2014. Vol. 20, № 4. P. 577–590.

21 Liu Y. et al. Source profiles of volatile organic compounds (VOCs) measured in China: Part I // Atmos Environ. 2008. Vol. 42, № 25. P. 6247–6260.

22 Zhang Y. et al. Levels, sources and health risks of carbonyls and BTEX in the ambient air of Beijing, China // Journal of Environmental Sciences. 2012. Vol. 24, № 1. P. 124–130.

23 Moliner-Martínez Y. et al. Study of the influence of temperature and precipitations on the levels of BTEX in natural waters // J Hazard Mater. 2013. Vol. 263. P. 131–138.

24 Liu K. et al. Aircraft measurements of BTEX compounds around Beijing city // Atmos Environ. 2013. Vol. 73. P. 11–15.

25 Mullaugh K.M. et al. Temporal and spatial variability of trace volatile organic compounds in rainwater // Chemosphere. Elsevier Ltd, 2015. Vol. 134. P. 203–209.

26 Jiang Z. et al. Seasonal and diurnal variations of BTEX compounds in the semi-urban environment of Orleans, France // Science of the Total Environment. Elsevier B.V., 2017. Vol. 574. P. 1659–1664.

27 Li L. et al. Pollution characteristics and health risk assessment of benzene homologues in ambient air in the northeastern urban area of Beijing, China // J Environ Sci (China). 2014. Vol. 26, № 1. P. 214–223.

28 Dehghani M. et al. Characteristics and health effects of BTEX in a hot spot for urban pollution // Ecotoxicol Environ Saf. Academic Press, 2018. Vol. 155. P. 133–143.

29 Ibragimova O.P. et al. Seasonal and spatial variation of volatile organic compounds in ambient air of almaty city, Kazakhstan // Atmosphere (Basel). MDPI, 2021. Vol. 12, № 12.

30 Sarafraz-Yazdi A. et al. Comparative study of the three sol-gel based solid phase microextraction fibers in extraction of BTEX from water samples using gas chromatography-flame ionization detection // Analytical Methods. 2010. Vol. 2, № 6. P. 746–752.

31 Varona-Torres E. et al. The Characterization of BTEX in Variable Soil Compositions Near Unconventional Oil and Gas Development // Advances in Chemical Pollution, Environmental Management and Protection. Elsevier B.V., 2017. Vol. 1. P. 321–351.

32 Do D.H. et al. Airborne volatile organic compounds in urban and industrial locations in four developing countries // Atmos Environ. Elsevier Ltd, 2015. Vol. 119. P. 330–338.

33 Tiwari V., Hanai Y., Masunaga S. Ambient levels of volatile organic compounds in the vicinity of petrochemical industrial area of Yokohama, Japan // Air Qual Atmos Health. 2010. Vol. 3, № 2. P. 65–75.

34 Miri M. et al. Investigation of outdoor BTEX: Concentration, variations, sources, spatial distribution, and risk assessment // Chemosphere. Elsevier Ltd, 2016. Vol. 163. P. 601–609.

35 Leusch F., Bartkow M. A short primer on benzene, toluene, ethylbenzene and xylenes (BTEX) in the environment and in hydraulic fracturing fluids. 2010.

36 Mustafa A. et al. BTEX removal in a modified free water surface wetland // Chemical Engineering Journal. Elsevier B.V., 2018. Vol. 333. P. 451–455.

37 Cavalcante R.M. et al. Development of a headspace-gas chromatography (HS-GC-PID-FID) method for the determination of VOCs in environmental aqueous matrices: Optimization, verification and elimination of matrix effect and VOC distribution on the Fortaleza Coast, Brazil // Microchemical Journal. 2010. Vol. 96, № 2. P. 337–343.

38 Е. А. Захаров С.Н.Ш. Экологические проблемы автомобильного транспорта: учеб. пособ / ed. ВолгГТУ. 2007. 107 p.

39 Skoog D.A., et al. "Principles of Instrumental Analysis. 6th ed. / ed. Thomson Brooks/Cole. 2007.

40 Dean J.R. Extraction methods for environmental analysis. John Wiley, 1998. 225 p.

41 Khajeh M., Zadeh F.M. Response surface modeling of ultrasound-assisted dispersive liquid-liquid microextraction for determination of benzene, toluene and xylenes in water samples: Box-behnken design // Bull Environ Contam Toxicol. 2012. Vol. 89, № 1. P. 38–43.

42 Sarafraz-Yazdi A., Khaleghi-Miran S.H., Es'haghi Z. Comparative study of direct immersion and headspace single drop microextraction techniques for btex determination in water samples using GC-FID // Int J Environ Anal Chem. 2010. Vol. 90, № 14. P. 1036–1047.

43 Hashemi M., Jahanshahi N., Habibi A. Application of ultrasound-assisted emulsification microextraction for determination of benzene, toluene, ethylbenzene and o-xylene in water samples by gas chromatography // Desalination. 2012. Vol. 288. P. 93–97.

44 Zhou Y.Y. et al. Application of portable gas chromatography-photo ionization detector combined with headspace sampling for field analysis of benzene, toluene, ethylbenzene, and xylene in soils // Environ Monit Assess. 2013. Vol. 185, № 4. P. 3037–3048.

45 Baltrėnas P. et al. Atmospheric BTEX concentrations in the vicinity of the crude oil refinery of the Baltic region // Environ Monit Assess. Kluwer Academic Publishers, 2011. Vol. 182, № 1–4. P. 115–127.

46 Chalabiani A., Matin A.A., Farhadi K. Zeolite-SiC in PVC matrix as a new SPME fiber for gas chromatographic determination of BTEX in water and soil samples // Journal of the Chinese Chemical Society. 2012. Vol. 59, № 9. P. 1080–1085.

47 Khajeh M. et al. Dispersive solid phase extraction combined with dispersive liquid-liquid extraction for the determination of BTEX in soil samples: Ant colony optimization-artificial neural network // J Chemom. John Wiley and Sons Ltd, 2015. Vol. 29, № 4. P. 245–252.

48 Dalvand K., Ghiasvand A. Simultaneous analysis of PAHs and BTEX in soil by a needle trap device coupled with GC-FID and using response surface methodology involving Box-Behnken design // Anal Chim Acta. Elsevier B.V., 2019. Vol. 1083. P. 119–129.

49 Sarafraz-Yazdi A. et al. New polypyrrole-carbon nanotubes-silicon dioxide solid-phase microextraction fiber for the preconcentration and determination of benzene, toluene, ethylbenzene, and o-xylene using gas liquid chromatography // J Sep Sci. Wiley-VCH Verlag, 2014. Vol. 37, № 18. P. 2605–2612.

50 Sarafraz-Yazdi A. et al. A novel solid-phase microextraction using coated fiber based sol-gel technique using poly(ethylene glycol) grafted multi-walled carbon nanotubes for determination of benzene, toluene, ethylbenzene and o-xylene in water samples with gas chromatography-flam ionization detector // J Chromatogr A. 2011. Vol. 1218, № 34. P. 5757–5764.

51 Li Q. et al. Evaluation of the solid-phase microextraction fiber coated with single walled carbon nanotubes for the determination of benzene, toluene,

ethylbenzene, xylenes in aqueous samples // J Chromatogr A. 2010. Vol. 1217, № 15. P. 2191–2196.

52 Nespeca M.G., Sequinel R., de Oliveira J.E. Ultra-fast gas chromatographic with flame ionization detector (UFGC-FID) and sonication methods for determination of total petroleum hydrocarbons fractions and BTEX in soil // Microchemical Journal. Elsevier Inc., 2019. Vol. 150.

53 Scheepers P.T.J. et al. Determination of exposure to benzene, toluene and xylenes in Turkish primary school children by analysis of breath and by environmental passive sampling // Science of the Total Environment. 2010. Vol. 408, № 20. P. 4863–4870.

54 Garcia de Freitas Junior G. et al. Simultaneous Voltammetric Determination of Benzene, Toluene and Xylenes (BTX) in Water Using a Cathodically Pre-treated Boron-doped Diamond Electrode // Electroanalysis. Wiley-VCH Verlag, 2019. Vol. 31, № 3. P. 554–559.

55 Zhang S. et al. Covalent organic frameworks as a novel fiber coating for solid-phase microextraction of volatile benzene homologues // Anal Bioanal Chem. Springer Verlag, 2017. Vol. 409, № 13. P. 3429–3439.

56 García Pinto C. et al. A simplified Quick, Easy, Cheap, Effective, Rugged and Safe approach for the determination of trihalomethanes and benzene, toluene, ethylbenzene and xylenes in soil matrices by fast gas chromatography with mass spectrometry detection // Anal Chim Acta. 2011. Vol. 689, № 1. P. 129–136.

57 Fernández E., Vidal L., Canals A. Zeolite/iron oxide composite as sorbent for magnetic solid-phase extraction of benzene, toluene, ethylbenzene and xylenes from water samples prior to gas chromatography□mass spectrometry // J Chromatogr A. Elsevier B.V., 2016. Vol. 1458. P. 18–24.

58 Behzadi M., Mirzaei M. Poly(o-anisidine)/graphene oxide nanosheets composite as a coating for the headspace solid-phase microextraction of benzene, toluene, ethylbenzene and xylenes // J Chromatogr A. Elsevier B.V., 2016. Vol. 1443. P. 35–42.

59 Assadi Y., Ahmadi F., Hossieni M.R.M. Determination of BTEX compounds by dispersive liquid-liquid microextraction with GC-FID // Chromatographia. 2010. Vol. 71, № 11–12. P. 1137–1141.

60 Rushi A.D. et al. Selective discrimination among benzene, toluene, and xylene: Probing metalloporphyrin-functionalized single-walled carbon nanotube-based field effect transistors // Journal of Physical Chemistry C. American Chemical Society, 2014. Vol. 118, № 41. P. 24034–24041.

61 Wang B. et al. A Highly Sensitive Diketopyrrolopyrrole-Based Ambipolar Transistor for Selective Detection and Discrimination of Xylene Isomers // Advanced Materials. Wiley-VCH Verlag, 2016. Vol. 28, № 21. P. 4012–4018.

62 Varona-Torres E. et al. Matrix-effect-free determination of BTEX in variable soil compositions using room temperature ionic liquid co-solvents in static headspace gas chromatography mass spectrometry // Anal Chim Acta. Elsevier B.V., 2018. Vol. 1021. P. 41–50.

63 Ghiasvand A., Zarghami F., Beiranvand M. Ultrasensitive direct determination of BTEX in polluted soils using a simple and novel pressure-controlled solid-phase microextraction setup // Journal of the Iranian Chemical Society. Springer Verlag, 2018. Vol. 15, № 5. P. 1051–1059.

64 Liu S. et al. Knitting aromatic polymers for efficient solid-phase microextraction of trace organic pollutants // J Chromatogr A. Elsevier B.V., 2016. Vol. 1450. P. 9–16.

65 Anbia M., Irannejad S. Modified SBA-15 mesoporous silica as a novel fiber coating in solid-phase microextraction and determination of BTEX compounds in water samples using gas chromatography-flame ionization detection // Analytical Methods. Royal Society of Chemistry, 2013. Vol. 5, № 6. P. 1596–1603.

66 Yu B. et al. BTEX in the environment: An update on sources, fate, distribution, pretreatment, analysis, and removal techniques // Chemical Engineering Journal. Elsevier B.V., 2022. Vol. 435.

67 Gao J. et al. Analysis of volatile organic compounds in environmental matrices by nitrogen-assisted headspace solid-phase extraction // New Journal of Chemistry. Royal Society of Chemistry, 2019. Vol. 43, № 22. P. 8788–8795.

68 Fakhari A.R. et al. A simple and rapid method based on direct transfer of headspace vapor into the GC injector: Application for determination of BTEX compounds in water and wastewater samples // Analytical Methods. 2012. Vol. 4, № 7. P. 1996–2001.

69 Song N. et al. Advances in pretreatment and analysis methods of aromatic hydrocarbons in soil // RSC Advances. Royal Society of Chemistry, 2022. Vol. 12, № 10. P. 6099–6113.

70 Varona-Torres E. et al. Matrix-effect-free determination of BTEX in variable soil compositions using room temperature ionic liquid co-solvents in static headspace gas chromatography mass spectrometry // Anal Chim Acta. Elsevier B.V., 2018. Vol. 1021. P. 41–50.

71 Arthur C.L., and P.Janusz. Solid Phase Microextraction with Thermal Desorption Using Fused Silica Optical Fibers. // Analytical Chemistry. 1990. Vol. 62, № 19. P. 2145–2148.

72 Pawliszyn J., Pawliszyn B., Pawliszyn M. Solid Phase Microextraction (SPME).

73 ZhouyaoZhangandJanuszPawliszyn.) Zhang, 2.; Pawliszyn // J. J. High Resolut. Ckromatogr. 1995. Vol. 67, № 2. 1477–1483 p.

74 Pawliszyn J. Theory of Solid-Phase Microextraction // Handbook of Solid Phase Microextraction. Elsevier Inc., 2012. P. 13–59.

75 Pawliszyn J. Handbook of solid phase microextraction. 478 p.

76 Nilsson T., Ferrari R., Facchetti S. Inter-laboratory studies for the validation of solid-phase microextraction for the quantitative analysis of volatile organic compounds in aqueous samples // Anal Chim Acta. Elsevier, 1997. Vol. 356, № 2–3. P. 113–123.

77 Ouyang G. Calibration // Handbook of Solid Phase Microextraction. Elsevier Inc., 2012. P. 167–199.

78 Spietelun A. et al. Understanding solid-phase microextraction: Key factors influencing the extraction process and trends in improving the technique // Chemical Reviews. 2013. Vol. 113, № 3. P. 1667–1685.

79 Pen A. et al. Trends in solid-phase microextraction for determining organic pollutants in environmental samples. 27–34 p.

80 Pawliszyn J. Solid-Phase Microextraction in Environmental Analysis // Encyclopedia of Analytical Chemistry. Wiley, 2000.

81 Dungan R.S. Headspace solid-phase microextraction (HS-SPME) for the determination of benzene, toluene, ethylbenzene, and xylenes (BTEX) in foundry molding sand // Anal Lett. 2005. Vol. 38, № 14. P. 2393–2405.

82 Brunton N.P., Cronin D.A., Monahan F.J. The effects of temperature and pressure on the performance of Carboxen/PDMS fibres during solid phase microextraction (SPME) of headspace volatiles from cooked and raw turkey breast // Flavour Fragr J. 2001. Vol. 16, № 4. P. 294–302.

83 Psillakis E. et al. Vacuum-assisted headspace solid phase microextraction: Improved extraction of semivolatiles by non-equilibrium headspace sampling under reduced pressure conditions // Anal Chim Acta. 2012. Vol. 742. P. 30–36.

84 Orazbayeva D. et al. Determination of transformation products of unsymmetrical dimethylhydrazine in water using vacuum-assisted headspace solid-phase microextraction // J Chromatogr A. Elsevier B.V., 2018. Vol. 1555. P. 30–36.

85 Dyussenkulova B.Zh. et al. Determination of nitrogen-containing pesticides in soil using vacuum-assisted headspace solid-phase microextraction // Chemical Bulletin of Kazakh National University. 1970. Vol. 110, № 4.

86 Zhakupbekova A., Baimatova N., Kenessov B. A critical review of vacuum-assisted headspace solid-phase microextraction for environmental analysis // Trends in Environmental Analytical Chemistry. Elsevier B.V., 2019. Vol. 22.

87 Mocho P., Desauziers V. Static SPME sampling of VOCs emitted from indoor building materials: Prediction of calibration curves of single compounds for two different emission cells // Anal Bioanal Chem. 2011. Vol. 400, № 3. P. 859–870.

88 Mocho P., Nicolle J., Desauziers V. Modelling of adsorption kinetics and calibration curves of gaseous volatile organic compounds with adsorptive solid-phase microextraction fibre: Toluene and acetone for indoor air applications // Anal Bioanal Chem. 2008. Vol. 392. P. 97–104.

89 Alam M.N., Ricardez-Sandoval L., Pawliszyn J. Numerical modeling of solid-phase microextraction: binding matrix effect on equilibrium time // Anal Chem. 2015. Vol. 87, № 19. P. 9846–9854.

90 Alam N. Insight into Quantitation of Solid-phase Microextraction. Ph.D. Thesis. Waterloo, ON, Canada: University of Waterloo, 2016.

91 Souza-Silva E.A. et al. Insights into the effect of the pdms-layer on the kinetics and thermodynamics of analyte sorption onto the matrix-compatible spme coating // Anal Chem. 2017. Vol. 89, № 5. P. 2978–2985.

92 Alam Md.N. et al. Effect of transport parameters and device geometry on extraction kinetics and efficiency in direct immersion solid-phase microextraction // Anal Chem. 2018. Vol. 90, № 19. P. 11548–11555.

93 Kenessov B. et al. Optimization of time-weighted average air sampling by solid-phase microextraction fibers using finite element analysis software // Molecules. Preprints, 2018. Vol. 23, № 11. P. 2736.

94 Kenessov B. et al. Analytica Chimica Acta Modeling solid-phase microextraction of volatile organic compounds by porous coatings using fi nite element analysis // Anal Chim Acta. Elsevier Ltd, 2019. Vol. 1076. P. 73–81.

95 Alam M.N., Ricardez-Sandoval L., Pawliszyn J. Numerical Modeling of Solid-Phase Microextraction: Binding Matrix Effect on Equilibrium Time // Anal Chem. American Chemical Society, 2015. Vol. 87, № 19. P. 9846–9854.

96 Alam M.N. et al. Effect of Transport Parameters and Device Geometry on Extraction Kinetics and Efficiency in Direct Immersion Solid-phase Microextraction // Anal Chem. American Chemical Society, 2018. Vol. 90, № 19. P. 11548–11555.

97 Alam M.N., Ricardez-Sandoval L., Pawliszyn J. Calibrant Free Sampling and Enrichment with Solid-Phase Microextraction: Computational Simulation and Experimental Verification // Ind Eng Chem Res. American Chemical Society, 2017. Vol. 56, № 13. P. 3679–3686.

98 Koziel J., Jia M., Pawliszyn J. Air sampling with porous solid-phase microextraction fibers // Anal Chem. 2000. Vol. 72, № 21. P. 5178–5186.

99 Kenessov B. et al. Modeling solid-phase microextraction of volatile organic compounds by porous coatings using finite element analysis // Anal Chim Acta. Elsevier B.V., 2019. Vol. 1076. P. 73–81.

100 Wilke C.R., Chang P. Correlation of diffusion coefficients in dilute solutions // AIChE Journal. 1955. Vol. 1, № 2. P. 264–270.

101 Kenessov B. et al. Perspectives and challenges of on-site quantification of organic pollutants in soils using solid-phase microextraction // TrAC - Trends in Analytical Chemistry. Elsevier B.V., 2016. Vol. 85. P. 111–122.

102 Fuller E.N., Schettler P.D., Giddings J.Calvin. New method for prediction of binary gas-phase diffusion coefficients // Ind Eng Chem. 1966. Vol. 58, № 5. P. 18–27.

103 Wilke C.R., Lee C.Y. Estimation of Diffusion Coefficients for Gases and Vapors // Ind Eng Chem. 1955. Vol. 47, № 6. P. 1253–1257.

104 Hirschfelder J.O., Byron Bird R., Spotz E.L. The transport properties of gases and gaseous mixtures. II // Chem Rev. 1949. Vol. 44, № 1. P. 205–231.

105 Lugg G. a. Diffusion coefficients of some organic and other vapors in air // Anal Chem. 1968. Vol. 40, № 7. P. 1072–1077.

106 Tang M.J. et al. Compilation and evaluation of gas phase diffusion coefficients of reactive trace gases in the atmosphere: Volume 2. Diffusivities of organic compounds, pressure-normalised mean free paths, and average Knudsen numbers for gas uptake calculations // Atmos Chem Phys. 2015. Vol. 15, № 10. P. 5585–5598.

107 Poling B.E., Prausnitz J.M., O'Connell J.P. The properties of gases and liquids, Fifth Edition // AIChE Journal. 2001. Vol. 24, № 6.

108 Sharma J., Tewari K., Arya R.K. Diffusion in polymeric systems–A review on free volume theory // Prog Org Coat. Elsevier, 2017. Vol. 111, № April. P. 83–92.

109 Zielinski J.M., Duda J.L. Predicting polymer/solvent diffusion coefficients using free-volume theory // AIChE Journal. 1992. Vol. 38, № 3. P. 405–415.

110 Yampolskii Y., Belov N. Investigation of Polymers by Inverse Gas Chromatography // Macromolecules. 2015. Vol. 48, № 19. P. 6751–6767.

111 Golay M.J.E. Theory of chromatography in open and coated tubular columns with round and rectangular cross-sections // Gas Chromatography / ed. Desty D.H. London: Butterworths, 1958. P. 36–55.

112 Pawliszyn J. Handbook of Solid Phase Microextraction. Elsevier Inc., 2012.

113 Martos P.A., Saraullo A., Pawliszyn J. Estimation of Air/Coating Distribution Coefficients for Solid Phase Microextraction Using Retention Indexes from Linear Temperature-Programmed Capillary Gas Chromatography. Application to the Sampling and Analysis of Total Petroleum Hydrocarbons in Air // Anal Chem. 1997. Vol. 69, № 3. P. 402–408.

114 Prikryl P., Sevcik J.G.K. Characterization of sorption mechanisms of solid-phase microextraction with volatile organic compounds in air samples using a linear solvation energy relationship approach // J Chromatogr A. 2008. Vol. 1179, № 1. P. 24–32.

115 Bolden A.L., Kwiatkowski C.F., Colborn T. New look at BTEX: are ambient levels a problem? // Environ Sci Technol. 2015. Vol. 49, № 9. P. 5261–5276.

116 Kenessov B. et al. Optimization of time-weighted average air sampling by solid-phase microextraction fibers using finite element analysis software // Molecules. Preprints, 2018. Vol. 23, № 11. P. 2736.

117 Ulrich S.; Brown, T.N.; Watanabe, N.; Bronner, G.; Abraham, M.H.; Goss, K.-U. N.; E. UFZ-LSER database v 3.2. Leipzig, Deutschland, Helmholtz Zentrum für Umweltforschung - UFZ, 2017.

118 Majer V., Svoboda V. Enthalpies of Vaporization of Organic Compounds: A Critical Review and Data Compilation. Oxford: Blackwell Scientific Publications, 1985.

119 Boscaini E. et al. Investigation of fundamental physical properties of a polydimethylsiloxane (PDMS) membrane using a proton transfer reaction mass spectrometer (PTRMS) // Int J Mass Spectrom. 2004. Vol. 239, № 2–3. P. 179–186.

120 Miller J.M. Chromatography: Concepts and Contrasts, 2nd Edition. Hoboken, New Jersey: Wiley, 2005.

121 Gustafson K.E., Dickhut R.M. Molecular Diffusivity of Polycyclic Aromatic Hydrocarbons in Air // J Chem Eng Data. 1994. Vol. 39, № 2. P. 286–289.

122 Erbil H.Y., Avci Y. Simultaneous Determination of Toluene Diffusion Coefficient in Air from Thin Tube Evaporation and Sessile Drop Evaporation on a Solid Surface // Langmuir. 2002. Vol. 18, № 13. P. 5113–5119.

123 Perry, R.H., Green D.W. Perry's Chemical Engineers' Handbook (8th ed.) // McGraw-Hill. 2008.

124 Kenessov B. et al. Modeling solid-phase microextraction of volatile organic compounds by porous coatings using finite element analysis // Anal Chim Acta. Elsevier Ltd, 2019. Vol. 1076. P. 73–81.

125 Chao K.-P. et al. Estimation of effective diffusion coefficients for benzene and toluene in PDMS for direct solid phase microextraction // Polym Test. Elsevier Ltd, 2011. Vol. 30, № 5. P. 501–508.

126 Cocchi G., de Angelis M.G., Doghieri F. Solubility and diffusivity of liquids for food and pharmaceutical applications in crosslinked polydimethylsiloxane (PDMS) films: I. Experimental data on pure organic components and vegetable oil // J Memb Sci. 2015. Vol. 492. P. 600–611.

127 Prikryl P., Sevcik J.G.K. Characterization of sorption mechanisms of solid-phase microextraction with volatile organic compounds in air samples using a linear solvation energy relationship approach // J Chromatogr A. 2008. Vol. 1179, № 1. P. 24–32.

128 Hayduk W., Laudie H. Prediction of diffusion coefficients for nonelectrolytes in dilute aqueous solutions // AIChE Journal. 1974. Vol. 20, № 3. P. 611–615.

129 Tyn M.T., Calus W.F. Diffusion coefficients in dilute binary liquid mixtures // J Chem Eng Data. 1975. Vol. 20, № 1. P. 106–109.

130 Mackay D., Leinonen P.J. Rate of evaporation of low-solubility contaminants from water bodies to atmosphere // Environ Sci Technol. 1975. Vol. 9, № 13. P. 1178–1180.

131 Liss P.S., Slater P.G. Flux of gases across the air-sea interface // Nature. 1974. Vol. 247. P. 181–184.

132 Southworth G.R. The role of volatilization in removing polycyclic aromatic hydrocarbons from aquatic environments // Bull Environ Contam Toxicol. 1979. Vol. 21, № 1. P. 507–514.

133 Jafari M., Ghalehsefidi M.J., Habibi S. Application of numerical simulation to solid phase-microextraction for decreasing of extraction time of Pyrene and Phthalate esters on solid coatings // J Chromatogr A. 2022. P. 463113.

134 Henry W. III. Experiments on the quantity of gases absorbed by water, at different temperatures, and under different pressures // Philos Trans R Soc Lond. 1803. Vol. 93. P. 29–274.

135 Wieland F. et al. Temperature dependence of Henry's law constants: An automated, high-throughput gas stripping cell design coupled to PTR-ToF-MS // Int J Mass Spectrom. 2015. Vol. 387. P. 69–77.

136 Schwarzenbach R.P., Gschwend P.M., Imboden D.M. Environmental Organic Chemistry, 3rd Edition. Wiley, 2016.

137 Fredenslund A., Gmehling J., Rasmussen P. Vapor-liquid Equilibria Using Unifac. Elsevier, 1977.

138 Popp P., Paschke A. Solid phase microextraction of volatile organic compounds using Carboxen-polydimethylsiloxane fibers // Chromatographia. 1997. Vol. 46, № 7–8. P. 419–424.

139 Kapar A. et al. Modeling the effect of temperature on solid-phase microextraction of volatile organic compounds from air by polydimethylsiloxane coating using finite element analysis // Anal Chim Acta. 2022. Vol. 1195. P. 339431.

140 Psillakis E. et al. Effect of Henry's law constant and operating parameters on vacuum-assisted headspace solid phase microextraction. // J Chromatogr A. Elsevier B.V., 2012. Vol. 1244. P. 55–60.

141 Mocho P., Desauziers V. Static SPME sampling of VOCs emitted from indoor building materials: Prediction of calibration curves of single compounds for two different emission cells // Anal Bioanal Chem. 2011. Vol. 400, № 3. P. 859–870.

142 Psillakis E. et al. Vacuum-assisted headspace solid phase microextraction: Improved extraction of semivolatiles by non-equilibrium headspace sampling under reduced pressure conditions // Anal Chim Acta. Elsevier B.V., 2012. Vol. 742. P. 30–36.

143 Yiantzi E., Kalogerakis N., Psillakis E. Vacuum-assisted headspace solid phase microextraction of polycyclic aromatic hydrocarbons in solid samples // Anal Chim Acta. 2015. Vol. 890. P. 108–116.

144 Zhakupbekova A. et al. Quantification of trace transformation products of rocket fuel unsymmetrical dimethylhydrazine in sand using vacuum-assisted headspace solid-phase microextraction // Environmental Science and Pollution Research. 2022.

145 Psillakis E. The effect of vacuum: an emerging experimental parameter to consider during headspace microextraction sampling // Anal Bioanal Chem. Springer, 2020. Vol. 412, № 24. P. 5989–5997.

146 Zhakupbekova A., Baimatova N., Kenessov B. Trends in Environmental Analytical Chemistry A critical review of vacuum-assisted headspace solid-phase microextraction for environmental analysis // Trends in Environmental Analytical Chemistry. Elsevier Inc., 2019. Vol. 22. P. e00065.

147 Muratuly A., Kapar A., Kenessov B. Modeling headspace solid-phase microextraction of volatile organic compounds from water samples with porous coatings using finite element analysis // Advances in Sample Preparation. Elsevier BV, 2022. Vol. 3. P. 100030.